

UNIVERSIDADE DE SÃO PAULO
FACULDADE DE ODONTOLOGIA DE BAURU

SUELEN PAINI

**F1 protein fraction obtained from latex incorporated into CaP-materials
improve critical-size defect bone repair in a concentration-dependent
manner**

BAURU

2018

SUELEN PAINI

F1 protein fraction obtained from latex incorporated into CaP-materials improve critical-size defect bone repair in a concentration-dependent manner

A fração proteica F1 obtida do látex incorporado à biomateriais a base de CaP melhora o reparo defeitos ósseos de tamanho crítico de maneira dependente da concentração

Dissertação constituída por artigo apresentada a Faculdade de Odontologia de Bauru da Universidade de São Paulo para obtenção do título de Mestre em Ciências no Programa de Ciências Odontológicas Aplicadas, na área de concentração Biologia Oral.

Orientador: Prof. Dr. Gerson Francisco de Assis.

BAURU

2018

Paini, Suelen

F1 protein fraction obtained from latex incorporated into CaP-materials improve critical-size defect bone repair in a concentration-dependent manner

86 p. : il. ; 31cm.

Dissertação (Mestrado) – Faculdade de Odontologia de Bauru.
Universidade de São Paulo

Orientador: Prof. Dr. Gerson Francisco de Assis

Autorizo, exclusivamente para fins acadêmicos e científicos, a reprodução total ou parcial desta dissertação/tese, por processos fotocopiadores e outros meios eletrônicos.

Assinatura:

Data:

Comitê de Ética da FOB-USP
Protocolo nº: 004/2017
DATA: 5/5/2017

(Cole a cópia de sua folha de aprovação aqui)

DEDICATÓRIA

Dedico essa dissertação...

Aos meus pais, Rosa e Roberto

Ao meu irmão Bruno

E aos mestres Dra. Tania, Dr. Gerson e Dr. Rumio.

AGRADECIMENTOS ESPECIAIS

Agradeço primeiramente a Deus, por me abençoar, iluminar a cada dia, me concedendo saúde, e disposição para concluir mais essa conquista em minha vida. Obrigada por mais esta vitória concedida. A Ele seja dada toda a honra e glória!

Ao meu querido pai, **Roberto Pains**, um pai zeloso, protetor, amável... obrigada por acreditar em mim, me acompanhar, apoiar e o incentivando incondicionalmente.

À minha amada mãe, **Rosa M. Moda Pains**, por ser fonte de vida, inspiração, amor, cuidado, proteção e por me fazer entender que nunca estarei sozinha ou desamparada, por acreditar em mim e me incentivar nos meus estudos e escolhas.

Agradeço vocês por me darem a vida, depois me ensinar a vivê-la com dignidade e responsabilidade, proporcionando todas as condições necessárias para o meu crescimento pessoal e profissional. Obrigada por se fazerem tão presente nos meus dias, mesmo a 70km de distância. Obrigada por todo esforço já feitos por mim, pois são vocês que nunca medem esforços para me ajudar. Obrigada pelos mimos, broncas, conselhos... por se preocuparem tanto comigo. Vocês ofereceram todo amor, carinho, apoio para eu chegar até aqui e o incentivo a prosseguir na jornada. Agradeço por tudo que vocês já me proporcionaram, pois, esta vitória também é de vocês! A vocês que amo infinitamente, não bastaria um muito obrigado. Agradeço também ao meu irmão, **Bruno Pains**, por me ajudar sempre que preciso, por torcer por mim e querer o meu sucesso, à sua esposa, **Glaucia C. Passareti Pains**, pela amizade e por me dar o primeiro e único sobrinho **João Vitor** que também sou grata ao meu lindo, por compartilhar momentos de alegria, brincadeira e amor. Mesmo com as dificuldades que encontramos no caminho, vocês, em momento algum, fizeram com que eu me sentisse sozinha no mundo. Sou eternamente grata a minha família e feliz por terem vocês comigo!!!

Agradeço ao meu namorado, **Rafael Di Salvo Arthur**, por estar comigo todo esse tempo e vivenciar cada momento destes últimos 2 anos de mestrado, ao meu lado, compartilhando alegrias, risadas, amor... Transformando meus dias de stress, nervosismo em momentos felizes. Obrigada por me ajudar sempre que preciso e não poderia deixar de agradecer por todos os “Gourmet” que você tem me proporcionado.

Ao meu orientador, **Dr. Gerson Francisco de Assis**, agradeço, por ter aceitado me orientar durante o mestrado, por transmitir tantos ensinamentos como orientador e durante suas aulas ministradas. Obrigada pela disponibilidade, paciência e pela credibilidade e oportunidade de realizar este trabalho... e por fornecer as ferramentas necessárias para a concretização desta pesquisa e principalmente, por acreditar em mim!

A **Dra. Tania Mary Cestari**, pelo seu imenso conhecimento, pela sua notável inteligência e calma, transmitidas em todas as nossas conversas. Exemplo de profissionalismo, por me ensinar o verdadeiro significado de uma pesquisa. Amadureci e cresci bastante nesses últimos anos e devo isso principalmente a ela, pelos ensinamentos que a mim foram transferidos. Muito obrigada pela confiança, apoio incondicional e pela competência. Gratidão pelo privilégio de desfrutar todo esse seu conhecimento.

Ao Prof. **Dr. Rumio Taga**, quem abriu as portas ao caminho da pesquisa, me orientou na iniciação científica e me abriu novos horizontes para que eu pudesse dar continuidade a vida acadêmica.

Aos professores **Dr. Gustavo P. Garlet** e **Dra. Camila O. R. Pegoraro**, por estarem sempre acessíveis, por compartilharem experiências e ensinamento durante o estágio PAE e durante as aulas ministradas.

Em especial ao **Departamento de Histologia de Ciências Biológicas**, onde encontrei pessoas amáveis, alegres, sempre de bem com a vida. Não poderia deixar de mencionar a incansável e admirável amiga e secretária do Departamento de Histologia, **Teresa Silva**, que estava sempre apta a ajudar em tudo que fosse possível, sempre com um sorriso no rosto e muito brilho. As técnicas de laboratório, **Daniele Ceolin** e **Patricia Germano**, obrigada por toda ajuda prestada com os procedimentos histológicos dessa pesquisa. A **D. Divina** por proporcionar todos os dias um delicioso chá/café para nós da histologia. Obrigada a vocês, pelo bom convívio e alegrias partilhadas

Aos amigos, **Paulinha S. Santos** e **Ricardo V. N. Arantes**, obrigada pelo apoio e ajuda de vocês desde da iniciação científica. Agradeço pelos momentos de aprendizados, conselhos e discussões enriquecedoras que colaboraram para o meu aprendizado. Obrigada pelo incentivo e exemplo de humildade e profissionalismo.

A **Ana Carolina C. Bighetti**, agradeço grandemente pelo esforço, dedicação, capricho e cuidado nesses últimos dias que me ajudou e por sempre ter sido prestativa.

Ao amigo **Ever Mena**, pela amizade e convívio durante este tempo, pela ajuda e sugestões.

AGRADECIMENTOS

Aos amigos, **Rafael Ortiz** e **Angélica Fonseca** pela amizade, carinho e atenção.

Aos queridos amigos da pós-graduação, **André Petenucci, Carolina Francisconi, Rodrigo Buzo, Jessica Melchiades, Micheli Soriani, Nádia Amôr, Nathália Lopes, Luan Macena, Luciana Saito, Dani P. Catanzaro, Priscila Colavite**....obrigada pela amizade, alegrias e conhecimentos compartilhados. E aos demais alunos da pós-graduação em Biologia Oral, por compartilharam comigo aulas, trabalhos e estudos.

Aos **alunos da graduação**, pela oportunidade de compartilhamento de saberes. Que todos os questionamentos, dúvidas que surgiram durante as monitorias, me motivaram a enfrentar este caminho de busca de maiores conhecimentos e atualidade.

Ao **corpo docente do Programa de mestrado em Ciências Odontológicas Aplicadas** e aos professores do **HRAC-USP** que nos enriqueceram com seus conhecimentos e aprendizados, comprometimento com o nosso crescimento. Aos **funcionários**, da Faculdade de Odontologia de Bauru, por me ajudaram em todos os momentos que eu precisei, pelo tratamento prestativo, acolhedor que sempre tiveram comigo

A **Dalva Ribeiro**, por estar sempre disponível e auxiliar nas minhas dúvidas com atenção e dedicação.

A **Dra. Dulce Constantino**, que contribuiu na construção do meu conhecimento durante a graduação e pela dedicação e prestação quando precisei da sua ajuda durante o mestrado.

Aos **membros da banca**, por aceitarem o convite e contribuir com o meu trabalho.

A todos os **amigos e familiares** que torceram por mim e pelo meu sucesso. Sem o apoio de vocês esse trabalho não seria possível.

Chego ao final desses agradecimentos com a sensação de que sou grandemente abençoada por Deus, pois é um privilégio estar nesta faculdade tão bem conceituada, rodeada de pessoas especiais e com uma família que meu deu base, apoio...permitindo que mais essa conquista se concretizasse hoje. O meu muito obrigada a todos!!!

AGRADECIMENTOS INSTITUCIONAIS

À **Faculdade de Odontologia de Bauru (FOB) – USP**, representada pelo excelentíssimo Diretor Prof. Dr. Carlos Ferreira dos Santos

Ao Departamento de Ciências Biológicas, **Disciplina de Histologia** da Faculdade de Odontologia de Bauru da Universidade de São Paulo.

À **Coordenação de aperfeiçoamento de Pessoal de Nível Superior (CAPES)** pela concessão da bolsa de estudo de Mestrado.

MUITO OBRIGADA.

Só os que não fazem nada nunca erram.

Teilhard de Chardin

ABSTRACT

One strategy for bone regenerative engineering is to use matrices associated to osteogenic and angiogenic molecules to increase bone formation. The aim of the present study was to evaluate the efficacy of treatment of extensive cranial bone defects with the F1 protein obtained from latex adsorbed at different concentrations (0,01%, 0,025%, 0,05% e 1%) to two different bone-substitutes biomaterials, deproteinized bovine bone (DBB) and biphasic calcium phosphate ceramics (pBCP) using a preclinical model in rats. Defects of 8-mm diameter were created in parietal bones of 72 rats filled with the pure biomaterial or carried with the different concentrations of F1 protein, in the microtomographic images a visual analysis of the microtomographic reconstructions of the skull through transverse, coronal and sagittal sections. Subsequently, the segmentation of the defect in the reconstructions will be done through an image processing algorithm to quantify the parameters. Analyzing, in the BP-G group, the total volume of bone (TV), in the CSBD-CG group, the total volume of new bone (TV-NB), and in the treated groups, the total volume of the grafted region (TV/GR), the total volume of new bone (TV-NB) and biomaterials (TV/DBB and TV/pBCP). In tissue sections stained with Hematoxylin and Eosin a descriptive histological analysis was performed to verify the tissue response to treatment with F1 protein and its association with osteoconductive biomaterial and correlate it with the histomorphometric determination to obtain percent values and volume of neoformed bone tissue, biomaterial, bone marrow and soft tissue. In the characterization of DBB and pBCP biomaterials, it was performed through the combined analytical methodology by SEM and SDD-EDS, to analyze external morphology and elemental chemical composition. All the results were compared between the groups by the ANOVA variance analysis and the Tukey tests at the 5% level of significance (Statistica v.5.1, StatSoft). After 12 weeks, defects treated with biomaterials without F1 presented greater bone formation in relation to the control group. The association of 0.025% and 0.05% of F1 plus DBB showed higher bone formation (32.6% and 25.1%, respectively) when compared to pBCP, being 19.3% and 15.1%, respectively. We conclude that the stimulation of angiogenesis and osteogenesis depends on its concentration of F1e and the physicochemical properties of the carrier material.

Key words: Bone Regeneration, Angiogenesis Inducers Agents, Biocompatible Materials, Rats.

RESUMO

Uma estratégia da engenharia regenerativa óssea é usar matrizes associadas a moléculas osteogênicas e angiogênicas para aumentar a formação óssea. O objetivo do presente estudo foi avaliar a eficácia do tratamento de defeitos ósseos cranianos extensos com a proteína F1 obtida do látex adsorvido em diferentes concentrações (0,01%, 0,025%, 0,05% e 1%) a dois diferentes biomateriais ósseo-substitutos, osso bovino desproteinizado (DBB) cerâmica de fosfato de cálcio bifásica (pBCP) utilizando um modelo pré-clínico em ratos. Defeitos de 8 mm de diâmetro foram criados nos ossos parietais de 72 ratos preenchidos com o biomaterial puro ou carregados com as diferentes concentrações da proteína F1, nas imagens microtomográficas uma análise visual das reconstruções microtomográficas do crânio através de cortes transversais, coronais e sagitais. Subsequentemente, foi feita segmentação do defeito nas reconstruções através de algoritmo de processamento de imagem para quantificação dos parâmetros. Analisando, no grupo BP-G, o volume total de osso (TV), no grupo CSBD-CG o volume total de osso novo (TV-NB), e nos grupos tratados, o volume total da região enxertada (TV-GR), volume total de osso novo (TV-NB) e biomaterial (TV-DBB e TV-pBCP). Nos cortes teciduais corados pela Hematoxilina e Eosina foi realizado uma análise histológica descritiva para verificar a resposta tecidual frente ao tratamento com a proteína F1 e a sua associação com biomaterial osteocondutor e correlaciona-la com a determinação histomorfométrica para a obtenção dos valores percentuais e de volume de tecido ósseo neoformado, biomaterial, medula óssea e tecido conjuntivo. Na caracterização dos biomateriais DBB e pBCP, foi realizado através da metodologia analítica combinada por SEM e SDD-EDS, para analisar morfologia externa e composição química elementar. Todos os resultados foram comparados entre os grupos pela análise de variância ANOVA e o teste de Tukey ao nível de significância de 5% (Statistica v.5.1, StatSoft). Após 12 semanas, defeitos tratados com biomateriais sem F1 apresentaram maior formação óssea em relação ao grupo controle. A associação de 0,025% e 0,05% de F1 mais DBB mostraram maior formação óssea (32,6% e 25,1%, respectivamente) quando comparados com pBCP, sendo 19,3% e 15,1%, respectivamente. Nós concluímos que, a estimulação da angiogênese e osteogênese depende de sua concentração de F1 e das propriedades físico-químicas do material carreador.

Palavras-chave: Regeneração Óssea, Indutores da Angiogênese, Materiais Biocompatíveis, Ratos.

LIST OF ABBREVIATIONS AND ACRONYMS

β-TCP	Beta-tricalcium phosphate
μA	Microampère
μm	Micrometer
®	Trademark
2D	Two-Dimensional
3D	Three-Dimensional
°C	Degrees Celsius
™	Trademark
μA	Microamp
ANOVA	Analisis of variance
B	Border
BCP	Biphasic calcium phosphate
BMP	Bone morphogenetic protein
BMP-2	Bone morphogenetic protein 2
BP-G	Bone-plug group
BV	Bone volume
BV/TV	Bone volume/Total Volume
C	Carbon
Ca	Calcium
cc	Cubic centimeter
CEEPA	Ethics Committee on Animal Education and Research at FOB-USP
CEVAP	Center for the study of venomous and venomous animals
CG	Control group
cm	Centimeter
CSBD	Critical size bone defects
CT	Connective tissue
DBB	Deproteinized bovine bone
DEAE-cellulose	Diethylaminoethyl cellulose
EDS	Energy dispersive spectroscopy
EDTA	Ethylenediamine tetraacetic acid

E.G.	Example
F1	Fraction 1
FBGCs	Large multinucleated foreign body giant cells
FGFs	Fibroblast growth factors
Fig.	Figure
FOB	Bauru school of dentistry
G	Group
GR	Grafted region
HA	Hydroxyapatite
HE	Hematoxylin and eosin
I.E.	In other words
IGFs	Insulin-like growth factor
IL-10	Interleukin-10
Inc.	Incorporated
kg	Kilogram
kV	Kilovolt
LB	Left border
Ltda.	Limited
M	Molar
MB	Marrow bone
Mg	Magnesium
mg	Milligram
Micro-CT	Microcomputed tomography
Min	Minutes
mL	Milliliter
mm	Millimeter
mm³	Cubic millimeter
n^o	Number
NaCl	Sodium chloride
NB	New bone
Nm	Nanometers
O	Oxygen
P	Phosphorus

p	Statistical p-value; descriptive level
pBCP70/30	Biphasic calcium phosphate 70/30
PDEM	Probability density evolution method
PDGF	Platelet-derived growth factor
pH	Hydrogenation potential
RB	Right border
rhBMP-2	Recombinant human bone morphogenetic protein 2
ROI	Region of interest
S	Section
SDD	Silicon drift detector
SEM	Scanning Electron Microscopy
SP	São Paulo
ST	Soft tissue
t	Test
TA	Total area
TAi	Total area of each structure
TC	Connective tissue
TCP	Tricalcium phosphate
TG	Treatment group
TV	Total volume
UNESP	Paulista state university “Júlio Mesquita Filho”
USA	United States of America
USP	University of São Paulo
V	Vessel
v	Volume
Vv	Volume density
v/v	Volume/volume
VEGF	Vascular endothelial growth factor
vs.	Versus
VT	Total volume
X	Volume density belonging to a given constituent

SUMMARY

1	INTRODUCTION	15
2	PROPOSITION	21
3	ARTICLE.....	25
4	DISCUSSION.....	61
5	CONCLUSION	67
	REFERENCES	71
	APPENDIX	81
	ANNEX.....	85

1 INTRODUCTION

1 INTRODUCTION

The reconstruction of large bone defects or critical size bone defects caused by trauma, infection, fracture nonunion, bone tumor resection and spinal deformities are a major challenge in regenerative medicine, especially for oral and maxillofacial surgeons (Cancedda *et al.*, 2007).

The autogenous bone remains as the gold standard for grafting because it has the three classic properties for bone regeneration and engineering. Osteogenesis is the capacity of synthesizing new bone by its bone cells. Osteoinductivity occurs due to the morphogens contained in the bone matrix which are capable of inducing the pluripotent mesenchymal cells to differentiate into osteoblasts. Osteoconductiveness is possible by the 3D structure of bone, it serves as a scaffold for migration, adhesion, osteoblasts differentiation and bone matrix synthesis on the surface (Tadic and Epple, 2004). However, a second surgical intervention for graft harvesting is necessary and this results in an increased patient's morbidity in addition to the limited amount of disponible tissue in the donor site (Laurencin *et al.*, 2006). Consequently, to these limitations numerous bone substitutes have been or are being developed as an alternative to the autogenous graft (Campana *et al.*, 2014) and currently, has been associated with factors of growth and / or osteoinducers (Chin *et al.*, 2005; Liu *et al.*, 2009; Li *et al.*, 2011) in the intention to potentiate the repair.

Vascularization is extremely important during the bone repair process, which can provide a bone source (Zimmerer *et al.*, 2017), the blood vessels are responsible for the distribution of oxygen, in addition to the transport of nutrients, cells (osteoblasts and osteoclast precursors) growth factors and cytokines. Among the growth factors, we have VEGF that has a direct stimulating effect on angiogenesis and also on the differentiation of osteoblasts (Marenzana and Arnett, 2013; Liu *et al.*, 2017) highlighting a link between the two cell types (endothelial cells and osteoblasts) and morphogenetic protein (BMP) that is capable of recruiting and inducing differentiation of undifferentiated mesenchymal cells into osteoblasts (Santos *et al.*, 2005).

In Brazil, products obtained from the rubber tree *Hevea brasiliensis*, a tree native to the Amazon River basin, has shown positive effects in several clinical situations due to its biocompatibility and angiogenic activity accelerating the cicatricial process without producing hypersensitivity response (Mrue *et al.*, 2004). The latex membrane was used in humans in the

reconstruction of tympani destroyed by chronic infections (Araujo *et al.*, 2012). Possessing bioactive and angiogenesis-inducing properties, the membrane was successfully used in treatment of chronic wounds in patients with diabetes. In all cases they presented a vigorous and healthy formation of new blood vessels, although healing has varied person to person according to age or other factors (Frade *et al.*, 2004).

At dissertation of Mauricio (2006) evaluated by DEAE chromatography cellulose obtained 3 fractions of the latex which denominated F1, F2 and F3. The angiogenic activity of the isolated fractions was evaluated in the chorio-allantoic membrane of chicken eggs *Gallus domesticus*. The F1 also showed greater activity on vascular permeability during the repair of dermal ulcers performed on rabbit ears. In another study, was assessed whether the F1 was able to stimulate human umbilical vein endothelial cells. In this case, Although F1 did not directly stimulated endothelial cells from human umbilical cord, it acted in angiogenesis indirectly through stimulation of growth factors by monocytes / macrophages stimulated, or other mechanisms not yet clear-cut. Already, Lamounier (2004) evaluated the production of inflammatory cytokines *in vitro* in culture of peripheral blood mononuclear cells induced by Membrane. Cells did not proliferate in the presence of membrane due to changes during processing, total serum and F2 did not change in lymphoproliferative response and cytokine production, whereas F1 led to an increase in IL-10.

Regarding to concentration of the protein to be used, the F1 was incorporated in 4% carboxymethylcellulose gel (Bayer - São Paulo, SP) in 3 different concentrations: 0.01%, 0.1% and 1% and applied on the ulcers on the ears of rabbits, showing that the concentration 0.01% of F1 was the most efficient to stimulate the healing of the lesion in a shorter time (Mendonça, 2004 and Mendonça *et al.*, 2010). Recently, the company Boticario has proposed a new anti-aging gel containing F1, able of restoring collagen production and skin elasticity. In a preclinical study with 60 women aged approximately 50 years, the use of F1 gel for 1 month led to a reduction of 80% in eye wrinkles and also the wrinkles in the forehead region, a study later confirmed with a larger group of 300 women.

In relation the application of F1 to bone repair, few studies have evaluated its potential, a preclinical study using latex in rat alveolar bone repair has shown that the latex was biocompatible and able of leading to a progressive osseointegration stimulating angiogenesis and accelerating the process of new bone formation in the first days of alveolar bone repair (Balabanian *et al.*, 2006). In another study, compared the osseointegration of the dental implant

(3.3 diameter x 10.0 mm length) in circumferential defects in dog jaws (5.0 diameter x 6.3 mm depth) treated with latex angiogenic proteins (2.5% collagen + 2.5% hyaluronic acid and 0.01% of the latex protein) versus autogenous bone, study did not show significant differences regarding bone formation and implant bone contact (Manfrin Arnez *et al.*, 2012).

Machado and collaborators, evaluated the repair of bone defects in the tibia of rats with fibrin sealant derived from snake venom (CEVAP) associated or not with BMP-2 and/or F1 at concentrations of 5 or 8µg, the results showed higher bone formation in the groups that used the BMP-2 and F1 in relation to the control (without treatment), being more favorable to BMP2. However, the use of fibrin showed better results in relation to defects without fibrin, but the association of fibrin with BMP-2 was the one that presented better results in the treatment of the tibial defect (Machado *et al.*, 2015). Was also evaluated the use of two different concentrations of BMP-2 (5µg/10µg) and (5µg/10µg) of F1 associated with or without the monoolein gel vehicle in the treatment of cranial bone defects of 6mm in diameter. After 4 weeks, they showed greater bone formation in the defects treated with the vehicle associated with higher protein concentration (10µg), being more favorable to BMP-2 (Issa *et al.*, 2012). In this sense, is important to emphasize that although rhBMP-2 is a potent growth factor for bone repair (Carreira *et al.*, 2014), has been reported to have collateral effects such as bloating, seroma and an increased risk of cancer when used at high dosages (Carragee *et al.*, 2013).

Another essential factor that determines success or failure during inductive bone grafts is the competence of the carrier material. A good carrier material must be biodegradable, biocompatible, and the measure that carrier is absorbed, there must be replacement with new bone tissue without allowing the bone site to be exceeded (Toriumi and Robertson, 1993). Several carriers are being used, they are made from metals, ceramics, polymers and composites. Natural or synthetic ceramics based on calcium phosphate have been used in various medical applications due to their mechanical resistance, biocompatibility, but with low biodegradability (Agrawal and Sinha, 2016) and should have also properties of osteointegration, osteoinduction (Moore *et al.*, 2001). In a recent study, biphasic ceramics of porous calcium phosphate in the ratio HA/TCPp 7:30, showed high osteoinduction power and osteoconduction in the bone repair process, promoting bone neoformation similar to autogenous bone (Santos *et al.*, 2018). In addition to the inorganic bone, studies show that they promote osteoconduction and have a slower resorption, being an alternative in bone repair therapy in the craniomaxillofacial region (Cestari *et al.*, 2009).

The products proposed in this project have as objective to evaluate and demonstrate the level of safety and efficacy of medical products for health, clarifying the type of interaction that different materials may present in front of the association with a protein of vegetable origin with potential osteo stimulating activity, becoming more an alternative to bone substitutes in current use in procedures to fill bone defects caused by trauma or pathologies.

2 PROPOSITION

2 PROPOSITION

The objective of this study was to evaluate whether F1 protein obtained from natural latex interferes positively or negatively in the vascularization and bone formation of critical-size bone defects and, if positive, the best concentrations of F1 and the type of carrier biomaterial have potential for future clinical applications.

3 ARTICLE

3 ARTICLE

J Biomed Mater Res B Appl Biomater..

F1 protein fraction obtained from latex incorporated into CaP-materials improve critical-size defect bone repair in a concentration-dependent manner

Suelen Paini¹, Rumio Taga¹ and Gerson Francisco de Assis¹

¹ *Department of Biological Sciences, Bauru School of Dentistry, University of São Paulo, Bauru, São Paulo, Brazil*

* To whom correspondence should be addressed Suelen Paini, Department of Biological Sciences, Bauru School of Dentistry, University of São Paulo, Av. Dr. Octavio Pinheiro Brisolla, 9-75, Vila Universitária, Bauru SP, Brazil. Tel: +55 1498833-8090; Email: suelenpaini@usp.br

Keywords: Bone Regeneration, Angiogenesis Inducers, Biocompatible Materials, Rats

Running title: biphasic ceramic

ABSTRACT

One strategy of bone regenerative engineering is to use matrices associated to osteogenic and angiogenic molecules to increase bone formation. This study evaluated the bone formation in the rat critical-size defects (CSBD) treated with deproteinized bovine bone (DBB-TG) and biphasic calcium-phosphate (pBCP-TG) incorporated with different concentrations of the angiogenic F1 protein fraction obtained of *Hevea brasiliensis* latex (without, 0.01%, 0.025%, 0.05% and 0.1%) after 12 weeks. The defects of control group (CSBD-CG) did not received treatment. 2D and 3D μ CT analyses were used to quantify the density and total volume of new bone, biomaterial and soft tissue. 2D-histomorphometric analysis was performed for qualitative and quantitative analysis. All treatments of DBB-TG and pBCP without F1 and with 0.01% and 0.025% of F1 showed higher new bone volume compared to CSBD-CG. In DBB-TG new bone volume was significantly higher when incorporate with 0.025% and 0.05% of F1 than others concentration and pBCP with and without F1. In pBCP-TG the incorporation of the F1 did not promote bone tissue gain compared to pBCP without F1 ($p>0.05$) and a significant bone reduction was observed with 0.1% of F1. Overall, the F1 incorporated to DBB significantly improve the bone regeneration dependent on its concentration in a standardized rat CSBD model.

KEYWORDS

Bone Regeneration, Angiogenesis Inducers, Biocompatible Materials, Rats

INTRODUCTION

Bone defects can heal spontaneously under suitable physiological environmental conditions due to its regeneration ability ¹. However large defects caused by malformation, infection, trauma and tumor resection represent the most difficult problem in contemporary reconstructive surgery because it size exceed the natural ability of bone repair ². Bone grafting is one of the most commonly used surgical methods to augment or

accelerate bone regeneration³. Autogenous is considered as the gold standard grafting material for treatment of bone defects because, it possesses all required properties for bone regeneration in term of osteoconduction, osteoinduction and osteogenesis⁴. But, it still has some disadvantages such as limitation in donor supply, pain and site morbidity of the donor⁵. To overcome these problems, synthetic or xenogenic bone substitutes biomaterials have been made and used in the orthopaedic and dentistry fields of bone regeneration. Natural or synthetic calcium phosphate (CaP) ceramics have been used in several surgical applications due to their mechanical resistance, biocompatibility and chemical similarity with the bone mineral phase⁶. The CaP-ceramics have excellent osteoconductive properties serving as a scaffold for bone growth during the early bone healing phase⁷. However, they generally do not possess osteoinductive properties necessary for the repair of large bone defects^{8,9}. Nowadays, efforts are therefore focused on developing mixed systems combining CaP-ceramic with active molecules for bone regeneration in order to improve the osteogenic potential of this bone substitute¹⁰.

Addition of active molecules such as growth factors is particularly interesting because of their ability to target specific cellular receptors and activating various cellular processes¹¹. Among factors involved in bone repair, bone morphogenetic protein (BMP), fibroblast growth factors (FGFs), vascular endothelial growth factor (VEGFs), insulin-like growth factor (IGFs) and platelet-derived growth factor (PDGF), are being used as therapeutic agents due to their capacities for stimulating osteoblast differentiation and osteogenesis and promotion of neovascularisation^{12,13}. Bone repair is a process dynamic and temporal that requiring osteogenesis and angiogenesis coordination at the site of repair¹⁴⁻¹⁶. The existence of a functional vascular network within the bone defect provides sufficient oxygen and nutrients for to sustain growth, differentiation and tissue functionality. On the other hand, the insufficiency or lack of vascularization can cause ischemia, cell death and even late healing^{17,18}.

The natural latex of the rubber tree *Hevea brasiliensis* has been shown to be biocompatible and able to stimulate angiogenic activity, accelerating the healing process without producing hypersensitivity^{19,20}. Recently, a protein fraction (F1) was extracted and purified from the natural latex showing promising results for

angiogenic stimulation and tissue repair in pre-clinical studies^{19,21,22}. Regarding the application of F1 for the bone defect regeneration, few studies have evaluated its therapeutic effects. In the study of Arnez²³, the bone formation, osseointegration and implant stability in circumferential bone defects treated with 0.01% F1 incorporated to collagen plus hyaluronic acid showed similar results to autogenous bone and blood clot treatments until 12 weeks. In cranial bone defects of 5-mm, autograft and allograft treatment with or without application of 5µg of F1-protein showed at 4 and 6 weeks a similar bone neof ormation and expression of osteogenic and angiogenic factors, but these values were superior to the control group²⁴. In other study using a same experimental model, the bone defect treated with 5µg of F1 showed similar bone formation to the control group at 2 and 6 weeks, but significantly lower compared to 5µg of BMP-2 treatment²⁵. However, neither of these studies evaluated the relationship between protein dose and regenerative efficacy on delivery system.

The goal of the present study was to evaluate the dose-response of F1 carried to two different CaP-ceramics in the repair of skull critical-size bone defects. Thus, the amount of ceramic carrier, new formed bone and soft tissues present in the treated defects at 12 weeks after experimental surgeries was evaluated by traditional microscope 2D-histomorphometric analysis and modern 3D-microcomputed tomographic (µCT) morphometry. We hypothesized that physical-chemical characteristics of CaP-ceramic interferes with F1 adsorption/incorporation and bioavailability of the F1 leading to bone regeneration or fibrosis of large bone defect.

MATERIALS AND METHODS

Obtaining F1-protein and adsorption on biomaterials: Natural latex was extracted from *Hevea brasiliensis* tree clone RRMI-600 and stabilized with 0.5–2% ammonium hydroxide (Fig. 1A). In the Neurochemistry Laboratory of the Biochemistry and Immunology Department of the Ribeirão Preto, Medicine School, University of São Paulo, the ammonium-preserved latex was mixed in 2% acetic acid in a ratio of 1:2 v/v at pH5.0. After 30 min, the serum fraction of the latex was obtained (Fig.1B) and diluted in distilled water (1:1 v/v). The pH was

elevated to 9.0 with addition of sodium hydroxide (Fig. 1C). Three protein fractions (F1, F2 and F3) were obtained for chromatography on DEAE-cellulose (Fig. 1D) at room temperature and eluted with ammonium bicarbonate 0.01M with increase concentration gradient of NaCl (0.15M; 0.25M and 1.5M). The material was collected under a flux of 7mL/min and monitored for absorbance at 280nm. Peak I fraction (F-1) was then submitted to distilled water dialysis, lyophilization and storage at -20°C (Fig.1E) for subsequent adsorption into biomaterials (Fig.1F).

Incorporation of the F1 to the carriers

Carriers: The carriers used in this study were the sintered deproteinized bovine bone (DBB-TG) (Gen-Ox[®]inorg, Baumer S.A., Mogi Mirim, SP, Brazil, registry ANVISA n° 103.455.00086, with granulation 0.5-1.0mm) and Biphasic calcium phosphate (pBCP70/30) composed of hydroxyapatite (HA) and beta-tricalcium phosphate (β -TCP) in a weight ratio of 70/30 (GenPhos XP[®] (Baumer S.A., Mogi Mirim, SP, Brazil, lot 4061690, with granulation 0.5-0.75mm). Five DBB and pBCP70/30 samples were evaluated by a combined analytical methodology composed by electron beam scanner (SEM) and X-rays analyzer (SDD-EDS, energy dispersive spectroscopy) (PDEM eXpress[™], ASPEX Corporation, Delmont-USA) for characterization of external topography/morphology and elemental chemical composition. The morphological characterization of pBCP by SEM showed an irregular surface morphology with micro sized pores/cavities, while the DBB presented regular and smooth surface (Fig. 2A). In high magnification (2.000X) both biomaterials showed area of the sintered bioceramic. Regarding to the EDS analysis, the graphic (Fig. 2B) for both biomaterials showed the peaks related to carbon (C), oxygen(O), phosphorus (P), magnesium (Mg) and calcium (Ca). It was also possible to determine the Ca/P ratio for DBB and pBCP samples, and the obtained value corresponds to 1.66 and 1.67, respectively.

Incorporation procedures: The pure F1 was dissolved in saline solution at concentration of the 0.01% (100mgF1/1000mL), 0.025% (200mgF1/800mL), 0.05% (400mgF1/800mL) and 0.1% (800mgF1/800mL) in the vacuum of the lyophilize for removal of air. Then, to incorporate the different concentrations of F1 into materials, 80cc of the carrier was added 200mL of the F1 solution and homogenized for approximately 5

minutes. It was then kept in a cold chamber receiving shaking every 2 hours for approximately 140 hours. Subsequently, the solutions were filtered by the simple filtration method and frozen at -70°C . The total protein of the filtered supernatant was determined by the Bradford method. The calculations for determining the percentage of incorporation of each concentration of F1 to the different carriers were realized by subtracting the concentration of F1 solution and total protein of the filtered supernatant. The mean of perceptual of F1 incorporation on the DBB was of 67.7% for pBCP and 96.3% for DBB varying the quantity of F1 in the defect per material.(see Table of Fig. 2C)

In vivo test

Animal and experimental design: The bone formation evaluation study was conducted on 72 male *Wistar* rats (*Rattus norvegicus*) aged 120 days provided by the Central Animal House of Bauru School of Dentistry, University of São Paulo. All animals received pelleted diet and water ad libitum. The experimental protocol followed “The Guiding Principles for the Care and Use of Animals”, according to the principles of the Declaration of Helsinki, and was approved by the Institutional Review Board for Animal Research of Bauru School of Dentistry – University of São Paulo (Process n°. CEEPA 027/2011).

Surgical procedures and experimental groups: The animal surgeries (Fig. 3) were performed under general anesthesia with intramuscular injection of ketamine (75mg/Kg; Dopalen AgriBrands Purina do Brasil Ltda. Paulínia – SP, Brazil) and xylazine (5mg/Kg; Anasedan AgriBrands Purina do Brasil Ltda.) followed by fronto-parietal trichotomy and disinfection with 10% povidone-iodine. A half-moon incision was made on the skull skin with a n° 10 surgical blade and the flap was raised posteriorly exposing the cranial surface. Using an 8mm diameter trephine bur under continuous irrigation with saline, a full-thickness defect was created in the parietal bones of each rat Fig. 3A-B). In bone-plug group (BP-G, n=6), the bone plug was maintained in de defect and the skull was collected immediately after surgery (Fig. 3B). These defects were used for determination of the total volume of bone lost by micro-CT analysis. In the treated groups (DBB-TG, n=30 and pBCP-TG, n=30) and critical-size bone defect control group (CSBD-CG, n=6), the bone plug was removed exposing the dura-mater. In DBB-TG and pBCP-TG, the defects were filled with 100 mm³ of biomaterials without F1 (n=6) or plus

0.01%, 0.05%, 0.025% and 0.1% of F1 (n=6 for each concentration) homogenized with cardiac puncture blood (Fig.3C) and in the CSBD-CG solely with 100 mm³ of blood clot (Fig. 3D), the flap was retracted in its original position and sutured with 4-0 black silk thread (Silk suture thread, 4-0 – Ethicon® - Johnson and Johnson®, Brazil). The postoperative care consisted of subcutaneous injection of non-steroidal anti-inflammatory flunixin meglumine (2.5 mg/Kg; Banamine*-Schering-Plough SA, Rio de Janeiro, Brazil) for 12-24 hours.

Sample collection and micro-CT procedures and analysis: After 0h (BP-G) and 12 weeks (DBB-TG, pBCP-TG and CSBD-CG) postoperative, the animals were killed with an overdose of a ketamine/xylazine mixture. The cranial vaults with the lining skin were collected and fixed in 10% phosphate-buffered formalin for 48 hours. The skulls were scanned using a commercially available microcomputed tomography system (SkyScan 1174; Bruker microCT, Kontich, Belgium). The samples were submitted to follow pattern scanning: X-rays tube potential of 50kV, beam current of 800µA, exposure of 9000ms, 180° rotation with step 0.73. The process of image reconstruction was performed using the SkyScan software NRecon with the same parameters for all specimens. Subsequently, the slides/images were aligned in the coronal, sagittal and transaxial planes using the software DataViewer (SkyScan 1174; Bruker microCT, Kontich, Belgium).

Morphometric parameters in 3D and 2D micro-CT coronal slides using CTAn program (Fig. 4A): A total of 350 slides/images of defect in 2D coronal view between proximal and distal borders were used for morphometric evaluation (Figs. 4A1-A2). The manual ROI was used for selected the defect region located between left and right borders of defect (Fig. 4A3). In the BP-G group defects, the total volume of bone removed surgically or bone lost (TV-bone lost) at 0h was determinate (red area in A3). In the defects of CSBD-G the total volume of new bone (TV-NB) was calculated after segmentation, the process of binarizing images to “bone” and “non-bone” using a “global threshold” which is applied to all samples in a study (A3). We used the visual comparison for compare segmented and grayscale images to confirm that the segmentation is representative of the “physiologic” structure of the bone. In treated groups the total volume of grafted region (TV-GR) and new bone (TV-NB) and biomaterial (TV-DBB and TV-pBCP), as well as volume density (%) of new bone (NB/TV) and biomaterials (DBB/TV or pBCP/TV) was determinate after segmentation.

Histological procedures: The analysis by microCT is a non-destructive technique for the sample which remains usable for other tests, such as, histological analysis. Thus, the samples were demineralized in EDTA a solution containing 4.13% tritriplex III (Merck KGaA, Darmstadt, Germany) and 0.44% sodium hydroxide, for a period of approximately 40 days. The specimens were histologically processed for embedding in Histosec® (paraffin enriched with polymers of the EMD Millipore - division of Merck KGaA, Darmstadt, Germany). Latero-lateral semi-serial 5- μ m thickness sections (intervals of 200 μ m) of all defects were obtained, adhered to silanized slide and stained with Hematoxylin-Eosin (HE) for light microscope histomorphometric evaluation.

2D-Histomorphometry using AxioVision program (Fig.4B): Five coronal cross-section of defect were obtained approximately at 1mm (S1), 2.5mm (S2), 4mm (S3), 5.5mm (S4) and 6.5mm (S5) of anterior border towards the posterior border as illustrated in the Figure 4B1 and B2. High resolution image of all defects was obtained using a digital camera MC200 and Axioscope microscope with objective of x4 (Carl Zeiss). The total area of defect in CSBD-CG (TA-CSBD) and grafted region in the treated groups (TA-GR) were evaluated surrounded manually the contour of plug removed (Fig. 4B3) and grafted area (Fig. 4B4), respectively. The total area of each structure (TA_i) was calculated; as shown in the figure 4B5 and 4B6. The volume density (V_v) of new bone (V_v-NB), biomaterials (V_v-DBB or V_v-pBCP), bone marrow (V_v-MB) and connective tissue (V_v-CT) was calculated by relation: $V_v = (TA_i \times 100) / (TA-CSBD \text{ or } TA-GR)$.

Comparison of 2D-micro-CT morphometry and histomorphometry: For comparison of micro-CT and histomorphometric quantifications we used the volume density data obtained for both methodologies. Thus, similar 2D micro-CT images were selected and the V_v of new bone (V_v-NB), biomaterials (V_v-DBB or V_v-pBCP) and soft tissue (V_v-ST) was calculated. The linear correlation between two variables (histomorphometry and micro-CT morphometry) was evaluated by Pearson correlation coefficient. The interpretation of the correlation coefficients was as follows: $r > 0.7$ = strong correlation, $r = 0.4-0.7$ moderate correlation, $r < 0.4$ = weak correlation ²⁶.

The data obtained for total volume and volume density were compared among groups by one-way analysis of variance (ANOVA), followed by the Tukey test for multiple comparisons between them, using the

software "Statistica v.5.1" (StatSoft Inc., Tulsa, USA). A value of $p < 0.05$ was taken to reject the null hypothesis, i.e. as the significance level.

RESULTS

Comparison insight volume density (%) of structures obtained by histomorphometry and microCT

The excellent quality of images obtained by micro-CT scanning and histological sections as well as the similarity of both images obtained by both techniques can be observed in the Figures 5A-B and 6A-B. In 2D-micro-CT the granules of DBB and pBCP showed more hyperdense than bone tissue while in histological sections the granules is represented by areas weak stained in purple (hematoxylin) and bone stained in magenta (eosin). Although, soft tissues (eg. connective tissue, bone marrow and tegument) were easily distinguishable in histological sections, in micro-CT slices these structures are represented by dark areas. In the Tables (Fig. 5C and 6C) were observed the results obtained for volume density of biomaterials, new bone and soft tissue in 2D-histological sections and co-localized 2D-micro-CT slices. In individual sections a small variability of values between techniques was verified. This variability was reduced on the average of the five images and in the total slice evaluated in 3D micro-CT analysis. The paired t test showed no statistical difference between mean values of volume density obtained in micro-CT and histological images and the Pearson's correlation coefficient suggested strong correlation between both techniques for bone formation (Figs. 5D2 and 6D2) and DBB material (Fig. 6D1), but moderate for pBCP. (Fig. 6D1).

Histomorphometric evaluations

The results obtained for morphological evaluation were represented in the figures 7 and 8A, while the data of volume density was presented in the table (Fig. 8B). In the CSBD-CG group (Fig. 7A) a small bone formation occurred in the border lesion occupying in mean $20.7 \pm 8.2\%$ of bone removed surgically. The remaining of bone defect was filled by fibrous connective tissue and structures of tegument that collapsed into the defects. In both experimental groups, DBB (Fig. 7B) and pBCP70/30 (Fig. 8A), the volume density of biomaterial implanted was similar for all defects (60mm^3) and remained statistically stable until 12 weeks

occupying in mean 40% of grafted area (see table of Figure 8B). But, a tendency of decreasing of pBCP granules (table of Fig. 8B) associated to presence of large multinucleated foreign body giant cells (FBGCs, see Fig. 8A) was observed at concentration of 0.05% and 0.1% of F1.

In all defects of DBB-TG (Fig. 7B) and pBCP-TG70/30 (Fig. 8A) the new bone formation was located at the edge of the defect and on the dura mater surface with total or partial entrapment of CaP-granules within new bone matrix. The good osseointegration of DBB (details in the Fig. 7B) and pBCP70/30 (details in the Figure 8A) was observed by direct contact between the new formed bone and material surface without interposition of connective tissue. However, the quantity and extension of new bone formed, as well as the osseointegration of CaP granules were significantly dependent of F1-concentration and the type of biomaterial carrier used. In DBB-TG a significant increase of 50% new bone density volume was observed when 0.025% F1 was incorporated to DBB alone (32.6% vs. 21.8%). However, a negative effect was verified on concentrations above 0.05% F1. Histologically, the incorporation of 0.1% F1 to DBB resulted in the formation of a fibrous connective tissue containing large and tortuous vessels in the spaces between DBB particles. In relation to pBCP-TG, although the new bone volume density in pBCP plus 0.01%F1 was 25% higher than pBCP without F1 any statistical differences were observed. Nevertheless, above these concentrations, a drastic decreasing of new bone volume density inversely proportional to the F1 concentration was observed in pBCP-TG. The new bone reduction was accompanied by the increase of fibrous connective tissue in the spaces between granules. Comparatively (Table of Fig. 8B), 0.025% and 0.05% of F1 incorporate to DBB showed a higher new bone volume density (32.6% and 25.1%, respectively) compared to those incorporated with pBCP (19.3% and 15.1%, respectively).

μCT volumetric evaluations

Tridimensional images of defects (Fig.9A) showed irregular and small bone formation surrounding the border and absence of bone tissue within the center of the defect in the CSBD-TG. In both treated groups, DBB-TG and pBCP-TG, the amount of biomaterial exceeds the thickness of the remaining parietal bones and bone plug removed surgically (BP-G). The total volume of grafted region in DBB-TG and pBCP-TG (Table of Fig. 9C)

was 99.8% higher (mean of 85 mm³) than bone lost or bone plug removed surgically (mean of 42.6 mm³). Although no statistical differences were observed between the grafted volumes, a significant reduction of 13.4% was observed in pBCP-TG incorporated with 0.1%F1 accompanied by reduction of 24.5% pBCP granules. The new bone volume in CSBD-TG was of 7.8 ± 1.8 mm³ and significantly smaller compared to all treatments of DBB-TG, but only in pBCP without F1 and with 0.01% and 0.025% in pBCP-TG. The influence of F1 concentration and biomaterial carrier in the bone formation can be clearly seen in the bidimensional images of defect near to dura-mater region (Fig. 9B) and in the obtained volumetric data (Table of Fig. 3C). In DBB-TG new bone volume was significantly higher when incorporate with 0.025% and 0.05% F1 than others concentration and pBCP with and without F1 (compare the images of Fig. 9B). In these F1 concentrations most of the spaces between the DBB granules were filled by bone tissue reducing 9.9% of space filled with soft tissue (dark/hipodense areas). In pBCP-TG the incorporation of the F1 did not promote bone tissue gain compared to pBCP without F1 ($p > 0.05$), but a significant reduction was observed with 0.1% of F1.

Discussion

The three major surgical strategies currently employed and developed to regenerate bone defects are use of bone graft substitutes, combination of bioactive molecules with a carrier and combination of cells and/or bioactive molecules with a carrier. The application of the strategy more appropriate for repair of bone defects depending on their severity. In a critical size bone defect a large portion of the bone is lost and it may limit the ingrowth of bone-forming cells due to insufficient nutritional supply of bone graft/materials, which resulted in a fibrous healing. The inclusion of active molecules that have the potential to stimulate angiogenesis could allow greater control of the bone-formation/remodeling. This is a first preclinical study that showed an increase of bone formation and bone repair in defects treated with F1-active molecules with angiogenic capacity ¹⁹ incorporated to DBB in a concentration dependent manner.

In the 8-mm cranial bone defect, the empty defects of CSBD-TG group showed limited bone formation at the defect edge and no formation within their center at 12 weeks. In this period only 20.7%

of the total volume of the defect ($7.8 \pm 1.8 \text{ mm}^3$) was filled with new bone mineralized matrix with similar density/maturity to remained bone tissue. In our previous study²⁷, these characteristics of non-closure of the defects were maintained until 180 days can be considered a critical-size bone defect²⁸. Although, 5-mm bilateral bone defect have been used as critical size defect model²⁹. A pilot study carried out in our laboratory showed spontaneous healing of a 5-mm bone defect in adult rats leading to closed of defect ($47.5 \pm 9.8\%$ at 12 weeks and $83.3 \pm 13.1\%$ at 24 weeks, data not included) considered as a subcritical size defect that can heal spontaneously. Additionally, the potential for interactions between two adjacent defects should be considered due to the proximity between them³⁰ and small parietal bone thickness separating both defects (mean of $0.77 \pm 0.04 \text{ mm}$).

The efficiency or not of F1 incorporated to CaP carrier to increase the process of bone repair was verified after 12 weeks of healing using two established methodologies, 2D and 3D μ CT morphometry and histological quantification with planimetric evaluations³¹. No statistical differences in new bone volume density and a strong correlation ($r=0.958$ for DBB-TG and 0.910 for pBCP-TG) using both techniques was observed. Thus, they provided a unique profile of bone regeneration within critical-size defects and the effects of F1 concentration plus material carrier.

In all defects, the bone formation was present at the edge of the defect and on the dura mater surface with total or partial entrapment of CaP-granules within bone matrix. In DBB and pBCP without F1 the new bone was higher compared to CSBD-CG indicating that both CaP-materials increases the bone gain in CSBD defects. These CaP-materials created an artificial bridge between the bony edges, prevented the collapse of the defect space and achieved the required volume in CSBD defects as observed in ours previous study²⁷ and by others with osteoconductive matrices^{32 33}The newly formed bone was in close contact with the DBB and pBCP surface without interposition of connective tissue showed the excellent osteoconductive characteristic of these materials as already observed in other studies²⁷. However, DBB and pBCP were not able to lead to CSBD closure until 12 weeks. The incorporation to them of osteogenic and/or angiogenic stimulating molecules such as BMP-2 and VEGF

has shown to increase the osteogenic capacity of these materials in animal models^{34 35} Nevertheless, recent studies have showed that the application of growth factors by adsorbing them superficially onto DBB not showed to promote new bone formation in CSBD because it only gives a short-term burst of BMP2 release^{36 37}. Similarly the F1 protein also increased the newly formed bone volume when incorporated with CaP-materials however, the quantity and extension of new bone formation, as well as the osseointegration of CaP granules were significantly dependent of F1-concentration and the type of biomaterial carrier used.

Thus, the incorporation of angiogenic F1 protein on DBB increased the new bone volume leading to total and partial CSBD closure. The DBB incorporated with 0.025% and 0.05% of F1 induced a bone gain superior to that of the bone lost or surgically removed. Although, DBB occupied 40.3% of grafted volume and newly formed bone occupies the spaces between granules promoting a vertical bone gain. On the other hand, F1-concentration above these no bone gain was observed. In pBCP-TG a tendency of higher bone formation was observed at 0.01% of F1, but concentrations superior led to gradual reduction on bone formation. Anomalous vessels and increase in the number of multinucleated giant cells (CGM) in the pBPC surface were observed when 0.1% of F1 was incorporated. This negative effect can be attributed to the high concentration of F1 adsorbed on this biomaterial. It is worth noting that the mean percentage of F1 incorporation on the DBB was of 67.7% and 96.3% for pBCP, consequently varying the quantity of F1 in the defect per material.

Comparatively, the use of supraphysiological or overdoses of recombinant human BMP-2 (rhBMP-2) carried in absorbable collagen sponge has been reported that causes multiple adverse effects in clinical use, including cervical swelling³⁸ osteoclast activation with bone resorption and cyst-like bone void formation³⁹ and and heterotopic bone formation⁴⁰. Thus, novel therapeutic strategies have focused on controlled delivery of growth factors from scaffold materials to promote better bone regeneration at the treated site^{41 42 43}.

Conclusion

Is one of the first studies that showed a dose and temporal response of bone regeneration using F1 delivered from CaP-materials scaffolds in an 8mm CSBD in rat model. In this model, doses of 25 to 50 µg of F1 regenerated significantly greater bone compared to CaP-materials without F1. On the other hand we propose a new standardized combination of 2D/3D micro-CT and histomorphometric methodologies for evaluation of bone regeneration in future preclinical study using rat critical size calvarial defect model. Plant products have been used in traditional medicine for many years, and their anti-inflammatory, anti-allergic and anti-infective properties are well-established ⁴⁴. Recent reports have indicated that these natural compounds also have angiogenesis-modulating effects ^{45 46 47}.

REFERENCES

1. Cameron JA, Milner DJ, Lee JS, Cheng J, Fang NX, Jasiuk IM. Employing the biology of successful fracture repair to heal critical size bone defects. *Curr Top Microbiol Immunol* 2013;367:113-32.
 2. Henkel J, Woodruff MA, Epari DR, Steck R, Glatt V, Dickinson IC, Choong PF, Schuetz MA, Hutmacher DW. Bone Regeneration Based on Tissue Engineering Conceptions - A 21st Century Perspective. *Bone Res* 2013;1(3):216-48.
 3. Dimitriou R, Jones E, McGonagle D, Giannoudis PV. Bone regeneration: current concepts and future directions. *BMC Med* 2011;9:66.
 4. Laurencin C, Khan Y, El-Amin SF. Bone graft substitutes. *Expert Rev Med Devices* 2006;3(1):49-57.
 5. Myeroff C, Archdeacon M. Autogenous bone graft: donor sites and techniques. *J Bone Joint Surg Am* 2011;93(23):2227-36.
 6. Maté-Sánchez de Val JE, Mazón P, Guirado JLC, Ruiz RA, Ramírez Fernández MP, Negri B, Abboud M, De Aza PN. Comparison of three hydroxyapatite/ β -tricalcium phosphate/collagen ceramic scaffolds: an in vivo study. *J Biomed Mater Res A* 2014;102(4):1037-46.
 7. Albrektsson T, Johansson C. Osteoinduction, osteoconduction and osseointegration. *Eur Spine J* 2001;10 Suppl 2:S96-101.
 8. Daculsi G, LeGeros R. Biphasic calcium phosphate (BCP) bioceramics: Chemical, physical and biological properties. *Encyclopedia of Biomaterials and Biomedical Engineering* 2006:1-1.
 9. Li Y, Chen SK, Li L, Qin L, Wang XL, Lai YX. Bone defect animal models for testing efficacy of bone substitute biomaterials. *J Orthop Translat* 2015;3(3):95-104.
 10. Verron E, Khairoun I, Guicheux J, Bouler JM. Calcium phosphate biomaterials as bone drug delivery systems: a review. *Drug Discov Today* 2010;15(13-14):547-52.
-

11. Bouyer M, Guillot R, Lavaud J, Plettinx C, Olivier C, Curry V, Boutonnat J, Coll JL, Peyrin F, Josserand V and others. Surface delivery of tunable doses of BMP-2 from an adaptable polymeric scaffold induces volumetric bone regeneration. *Biomaterials* 2016;104:168-81.
 12. Yun YR, Jang JH, Jeon E, Kang W, Lee S, Won JE, Kim HW, Wall I. Administration of growth factors for bone regeneration. *Regen Med* 2012;7(3):369-85.
 13. Krishnan L, Willett NJ, Guldberg RE. Vascularization strategies for bone regeneration. *Ann Biomed Eng* 2014;42(2):432-44.
 14. Carano RA, Filvaroff EH. Angiogenesis and bone repair. *Drug Discov Today* 2003;8(21):980-9.
 15. Hankenson KD, Dishowitz M, Gray C, Schenker M. Angiogenesis in bone regeneration. *Injury* 2011;42(6):556-61.
 16. Zimmerer RM, Jehn P, Kokemüller H, Abedian R, Lalk M, Tavassol F, Gellrich NC, Spalthoff S. In vivo tissue engineered bone versus autologous bone: stability and structure. *Int J Oral Maxillofac Surg* 2017;46(3):385-393.
 17. Cao L, Wang J, Hou J, Xing W, Liu C. Vascularization and bone regeneration in a critical sized defect using 2-N, 6-O-sulfated chitosan nanoparticles incorporating BMP-2. *Biomaterials* 2014;35(2):684-698.
 18. Marenzana M, Arnett TR. The Key Role of the Blood Supply to Bone. *Bone Res* 2013;1(3):203-15.
 19. Mendonça RJ, Maurício VB, Teixeira LeB, Lachat JJ, Coutinho-Netto J. Increased vascular permeability, angiogenesis and wound healing induced by the serum of natural latex of the rubber tree *Hevea brasiliensis*. *Phytother Res* 2010;24(5):764-8.
 20. Balabanian CA, Coutinho-Netto J, Lamano-Carvalho TL, Lacerda SA, Brentegani LG. Biocompatibility of natural latex implanted into dental alveolus of rats. *J Oral Sci* 2006;48(4):201-5.
-
-

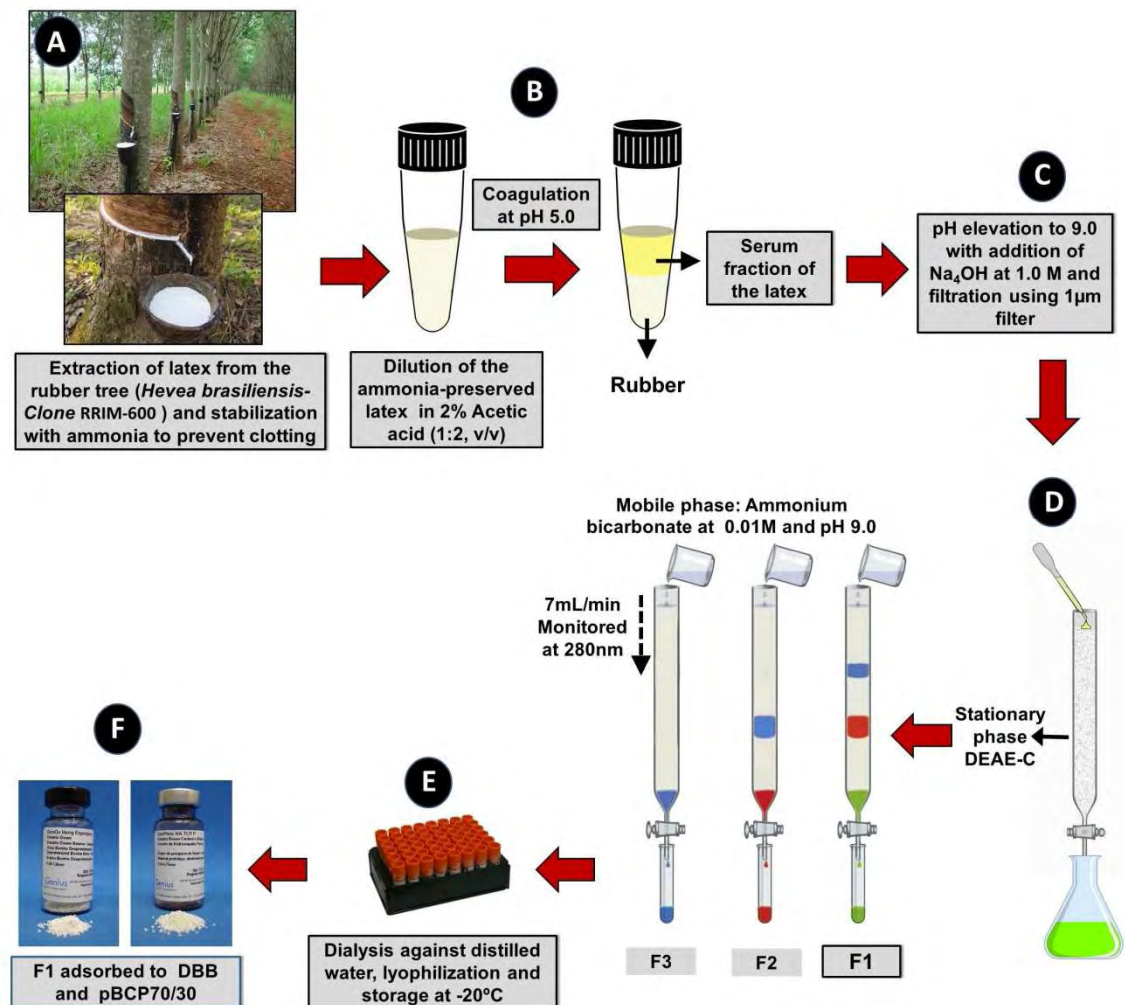
21. Sampaio RB, Mendonca RJ, Simioni AR, Costa RA, Siqueira RC, Correa VM, Tedesco AC, Haddad A, Coutinho Netto J, Jorge R. Rabbit retinal neovascularization induced by latex angiogenic-derived fraction: an experimental model. *Curr Eye Res* 2010;35(1):56-62.
 22. Ferreira M, Mendonça RJ, Coutinho-Netto J, Mulato M. Angiogenic properties of natural rubber latex biomembranes and the serum fraction of *Hevea brasiliensis*. *Brazilian Journal of Physics* 2009;39(3):564-569.
 23. Manfrin Arnez MF, Xavier SP, Pinto Faria PE, Pedrosa Júnior WF, Cunha TR, de Mendonça RJ, Coutinho-Netto J, Salata LA. Implant osseointegration in circumferential bone defects treated with latex-derived proteins or autogenous bone in dog's mandible. *Clin Implant Dent Relat Res* 2012;14(1):135-43.
 24. Santos Kotake BG, Gonzaga MG, Coutinho-Netto J, Ervolino E, de Figueiredo FAT, Issa JPM. Bone repair of critical-sized defects in Wistar rats treated with autogenic, allogenic or xenogenic bone grafts alone or in combination with natural latex fraction F1. *Biomed Mater* 2018;13(2):025022.
 25. Issa JP, Defino HL, Sebald W, Coutinho-Netto J, Iyomasa MM, Shimano AC, Bentley MV, Pitol DL. Biological evaluation of the bone healing process after application of two potentially osteogenic proteins: an animal experimental model. *Gerodontology* 2012;29(4):258-64.
 26. Holmes Jr L. *Concise Biostatistical Principles & Concepts: Guidelines for Clinical and Biomedical Researchers*: AuthorHouse; 2014.
 27. Rocha CA, Cestari TM, Vidotti HA, de Assis GF, Garlet GP, Taga R. Sintered anorganic bone graft increases autocrine expression of VEGF, MMP-2 and MMP-9 during repair of critical-size bone defects. *J Mol Histol* 2014;45(4):447-61.
 28. Spicer PP, Kretlow JD, Young S, Jansen JA, Kasper FK, Mikos AG. Evaluation of bone regeneration using the rat critical size calvarial defect. *Nat Protoc* 2012;7(10):1918-29.
-

29. Bosch C, Melsen B, Vargervik K. Importance of the critical-size bone defect in testing bone-regenerating materials. *J Craniofac Surg* 1998;9(4):310-6.
 30. Vajgel A, Mardas N, Farias BC, Petrie A, Cimões R, Donos N. A systematic review on the critical size defect model. *Clin Oral Implants Res* 2014;25(8):879-93.
 31. Park SY, Kim KH, Koo KT, Lee KW, Lee YM, Chung CP, Seol YJ. The evaluation of the correlation between histomorphometric analysis and micro-computed tomography analysis in AdBMP-2 induced bone regeneration in rat calvarial defects. *J Periodontal Implant Sci* 2011;41(5):218-26.
 32. Xu A, Zhuang C, Xu S, He F, Xie L, Yang X, Gou Z. Optimized Bone Regeneration in Calvarial Bone Defect Based on Biodegradation-Tailoring Dual-shell Biphasic Bioactive Ceramic Microspheres. *Sci Rep* 2018;8(1):3385.
 33. Beltrán V, Engelke W, Prieto R, Valdivia-Gandur I, Navarro P, Manzanares MC, Borie E, Fuentes R. Augmentation of intramembranous bone in rabbit calvaria using an occlusive barrier in combination with demineralized bone matrix (DBM): a pilot study. *Int J Surg* 2014;12(5):378-83.
 34. Wu G, Hunziker EB, Zheng Y, Wismeijer D, Liu Y. Functionalization of deproteinized bovine bone with a coating-incorporated depot of BMP-2 renders the material efficiently osteoinductive and suppresses foreign-body reactivity. *Bone* 2011;49(6):1323-30.
 35. Wernike E, Montjovent MO, Liu Y, Wismeijer D, Hunziker EB, Siebenrock KA, Hofstetter W, Klenke FM. VEGF incorporated into calcium phosphate ceramics promotes vascularisation and bone formation in vivo. *Eur Cell Mater* 2010;19:30-40.
 36. Schwarz F, Rothamel D, Herten M, Ferrari D, Sager M, Becker J. Lateral ridge augmentation using particulated or block bone substitutes biocoated with rhGDF-5 and rhBMP-2: an immunohistochemical study in dogs. *Clin Oral Implants Res* 2008;19(7):642-52.
-
-

37. Schmitt C, Lutz R, Doering H, Lell M, Ratky J, Schlegel KA. Bio-Oss® blocks combined with BMP-2 and VEGF for the regeneration of bony defects and vertical augmentation. *Clin Oral Implants Res* 2013;24(4):450-60.
38. Perri B, Cooper M, Laurysen C, Anand N. Adverse swelling associated with use of rh-BMP-2 in anterior cervical discectomy and fusion: a case study. *Spine J* 2007;7(2):235-9.
39. Zara JN, Siu RK, Zhang X, Shen J, Ngo R, Lee M, Li W, Chiang M, Chung J, Kwak J and others. High doses of bone morphogenetic protein 2 induce structurally abnormal bone and inflammation in vivo. *Tissue Eng Part A* 2011;17(9-10):1389-99.
40. Axelrad TW, Steen B, Lowenberg DW, Creevy WR, Einhorn TA. Heterotopic ossification after the use of commercially available recombinant human bone morphogenetic proteins in four patients. *J Bone Joint Surg Br* 2008;90(12):1617-22.
41. Brown KV, Li B, Guda T, Perrien DS, Guelcher SA, Wenke JC. Improving bone formation in a rat femur segmental defect by controlling bone morphogenetic protein-2 release. *Tissue Eng Part A* 2011;17(13-14):1735-46.
42. Kolambkar YM, Boerckel JD, Dupont KM, Bajin M, Huebsch N, Mooney DJ, Hutmacher DW, Goldberg RE. Spatiotemporal delivery of bone morphogenetic protein enhances functional repair of segmental bone defects. *Bone* 2011;49(3):485-92.
43. Guda T, Darr A, Silliman DT, Magno MH, Wenke JC, Kohn J, Brown Baer PR. Methods to analyze bone regenerative response to different rhBMP-2 doses in rabbit craniofacial defects. *Tissue Eng Part C Methods* 2014;20(9):749-60.
44. Recio MC, Andujar I, Rios JL. Anti-inflammatory agents from plants: progress and potential. *Curr Med Chem* 2012;19(14):2088-103.
-
-

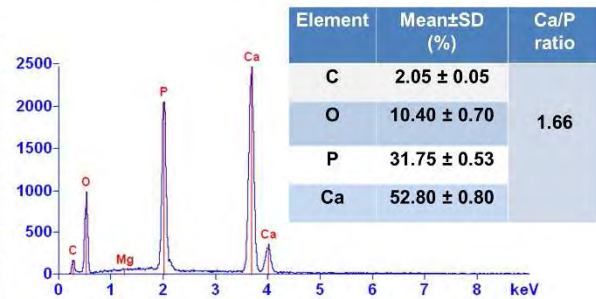
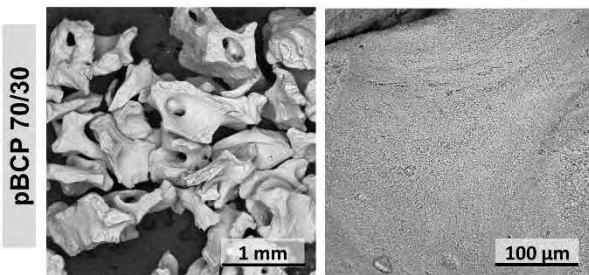
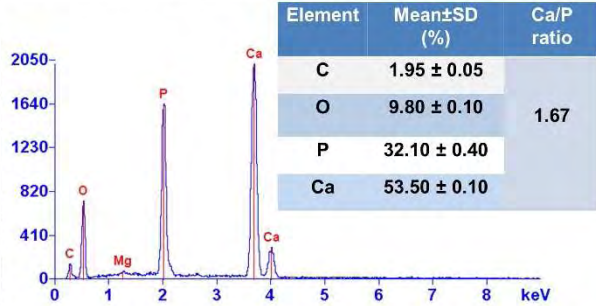
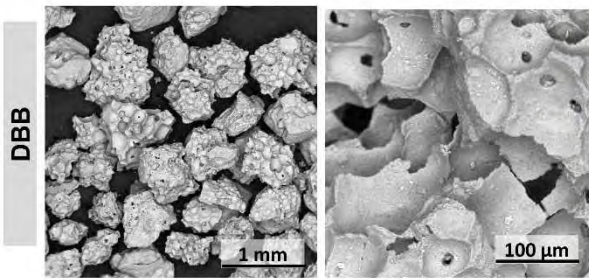
45. Sagar SM, Yance D, Wong RK. Natural health products that inhibit angiogenesis: a potential source for investigational new agents to treat cancer-Part 1. *Curr Oncol* 2006;13(1):14-26.
46. Wen W, Lu J, Zhang K, Chen S. Grape seed extract inhibits angiogenesis via suppression of the vascular endothelial growth factor receptor signaling pathway. *Cancer Prev Res (Phila)* 2008;1(7):554-61.
47. Lu K, Chakroborty D, Sarkar C, Lu T, Xie Z, Liu Z, Basu S. Triphala and its active constituent chebulinic acid are natural inhibitors of vascular endothelial growth factor-a mediated angiogenesis. *PLoS One* 2012;7(8):e43934.
-
-

LIST OF FIGURES



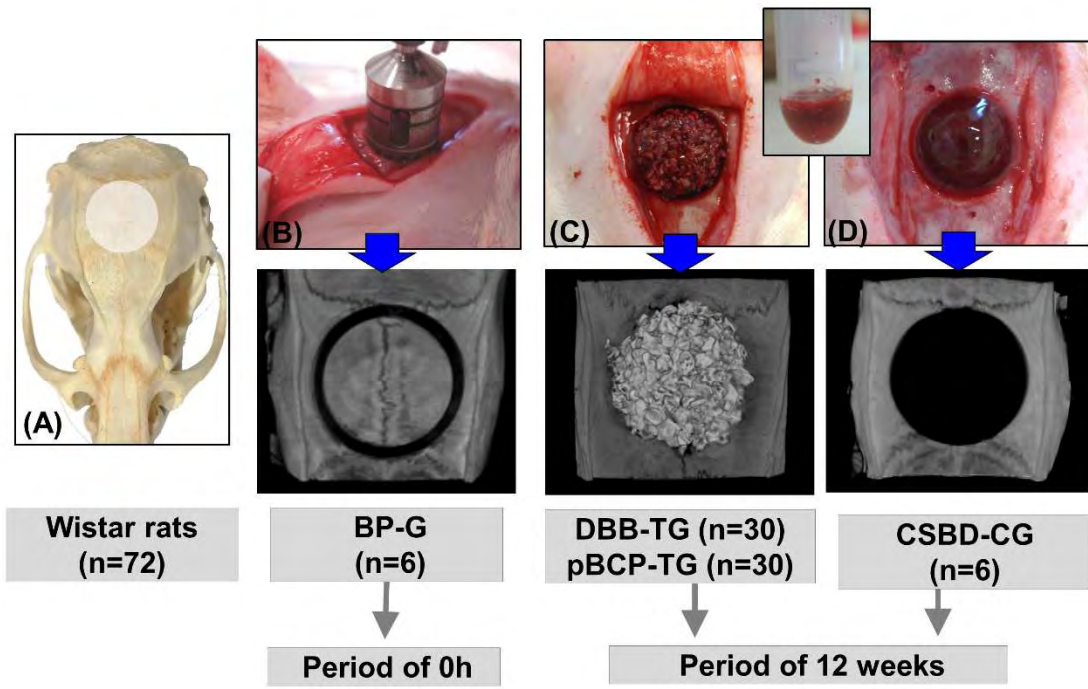
(A) SEM photomicrography

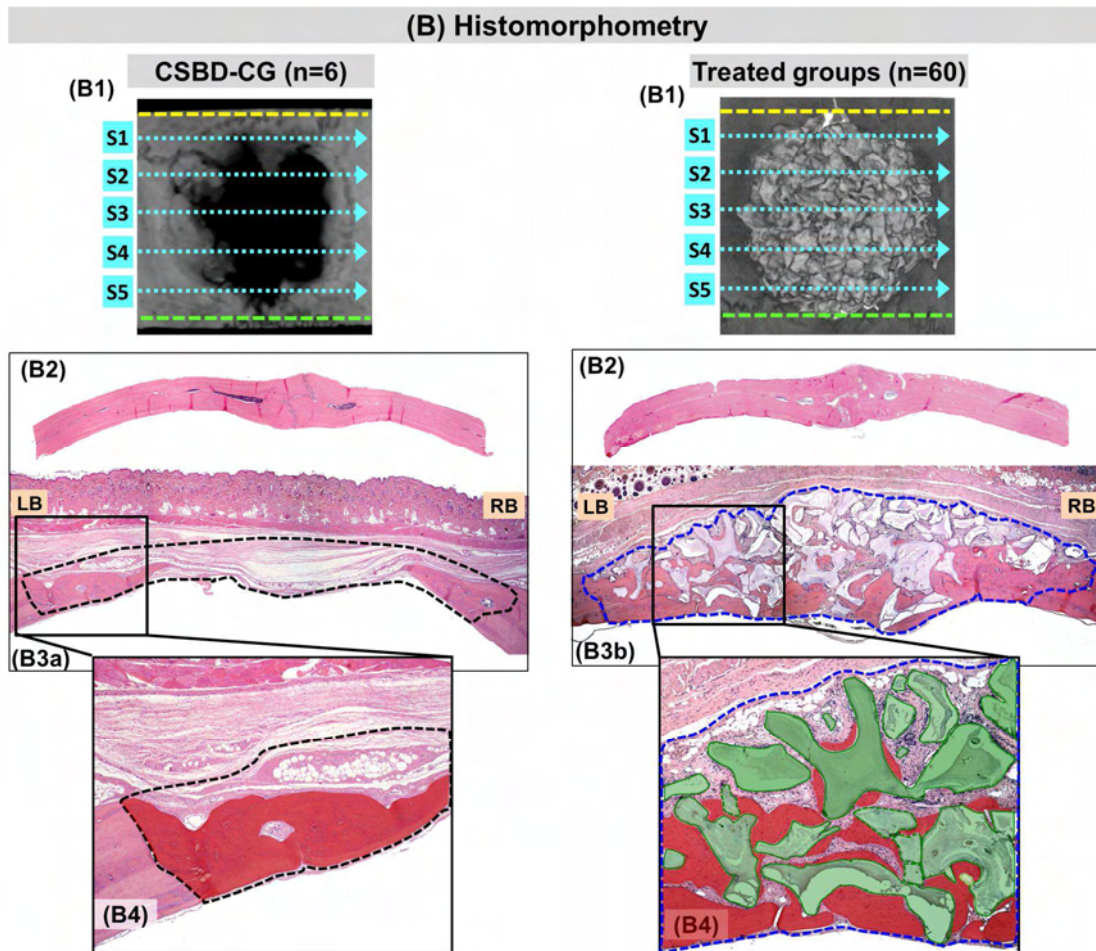
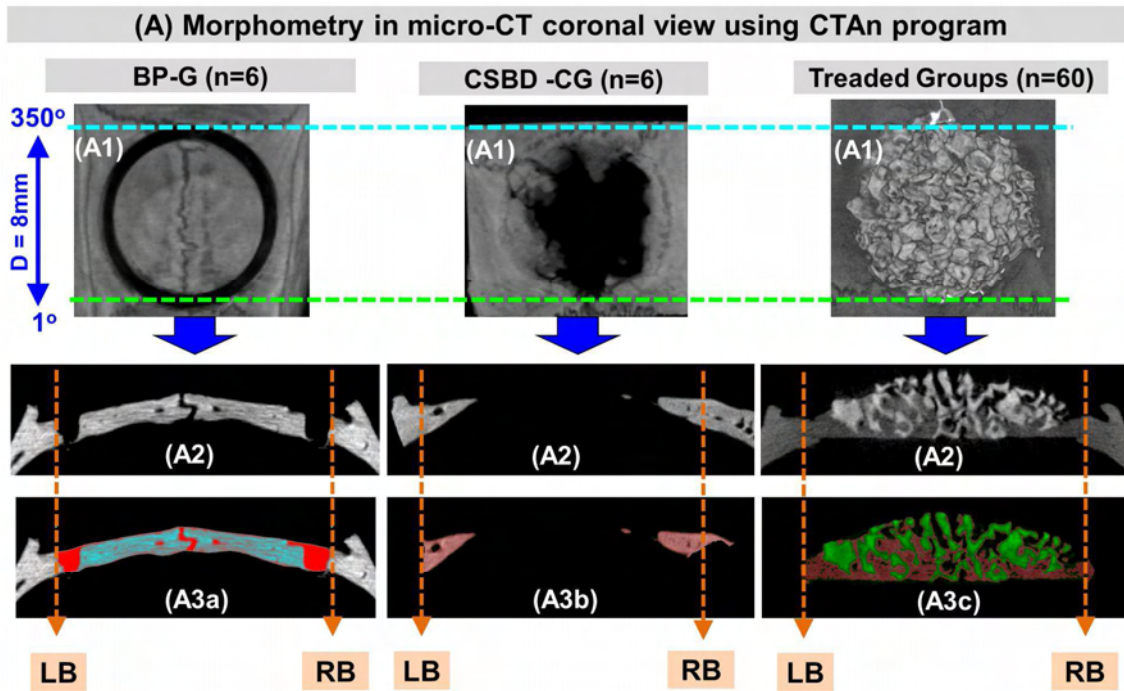
(B) Energy-dispersive X-ray spectroscopy (EDS)

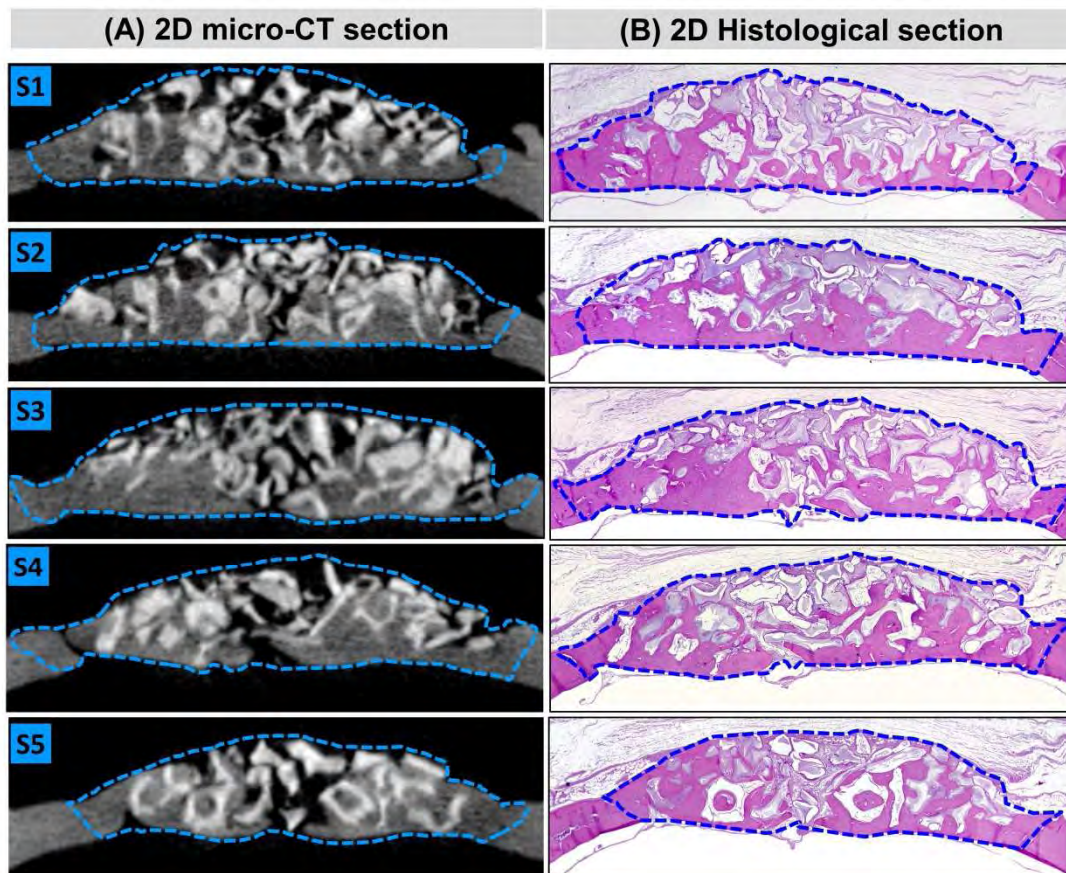


(C) F1-incorporation on the CaP-materials and F1-concentration implanted in the defect

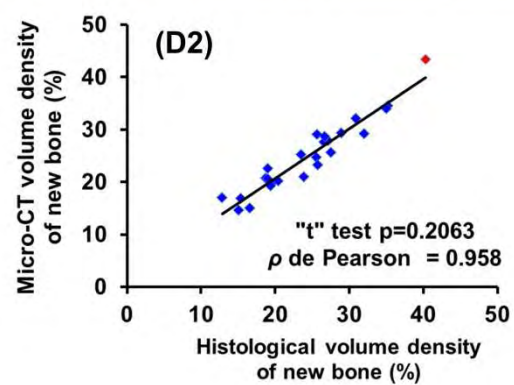
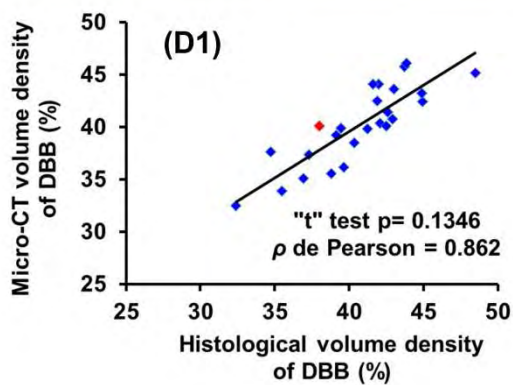
F1 solution (%)	F1 incorporation on the CaP-materials				F1 implanted/defect	
	Percentual of F1 incorporated (%)		Concentration of F1 incorporate (μg/cc)		Concentration F1(mg)/80mg of biomaterial	
	DBB	pBCP	DBB	pBCP	DBB	pBCP
0.01	65.7	94.6	131	189	11	15
0.025	65.0	99.09	325	495	26	40
0.05	66.0	95.98	660	958	53	77
0.1	74.3	95.61	1480	1910	118	153

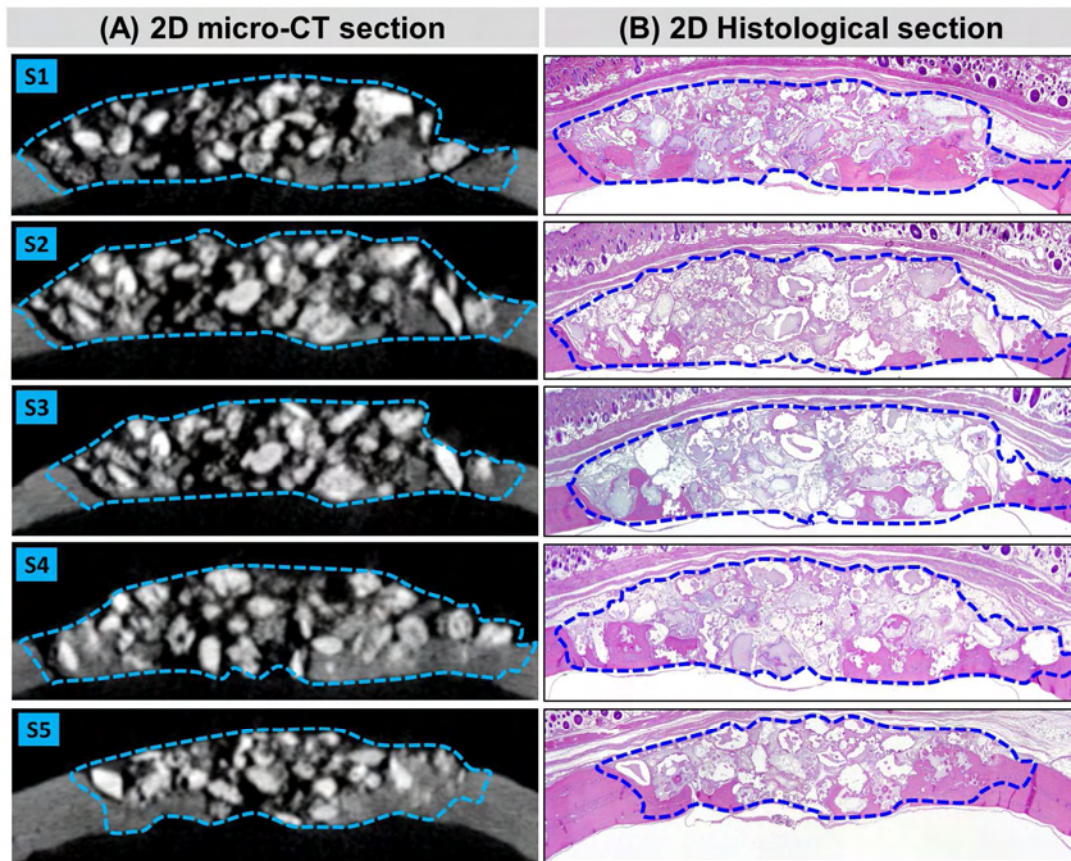




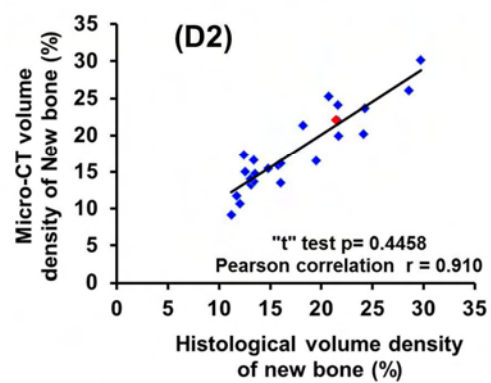
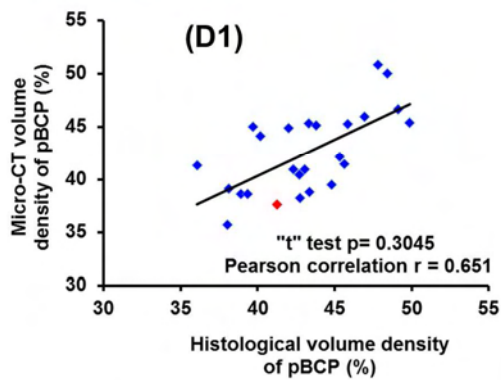


Slice/ Section	(C) Volume density (%)					
	DBB		New Bone		Soft tissue	
	Micro-CT	Histo	Micro-CT	Histo	Micro-CT	Histo
1	36.62	42.88	41.02	37.45	22.36	19.67
2	39.96	39.50	48.17	46.21	11.87	14.29
3	40.64	43.14	44.73	43.98	14.63	12.88
4	38.09	36.29	43.19	38.27	18.72	25.44
5	34.69	38.55	39.46	36.07	25.85	23.38
Mean ± SD	38.0 ± 1.9	40.1 ± 2.4	43.3 ± 2.5	40.4 ± 3.8	18.7 ± 4.3	19.5 ± 4.8
350 slice	39.5	-	43.4	-	19.8	-

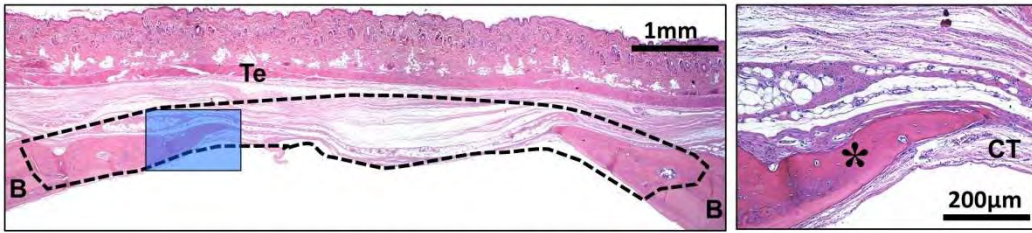




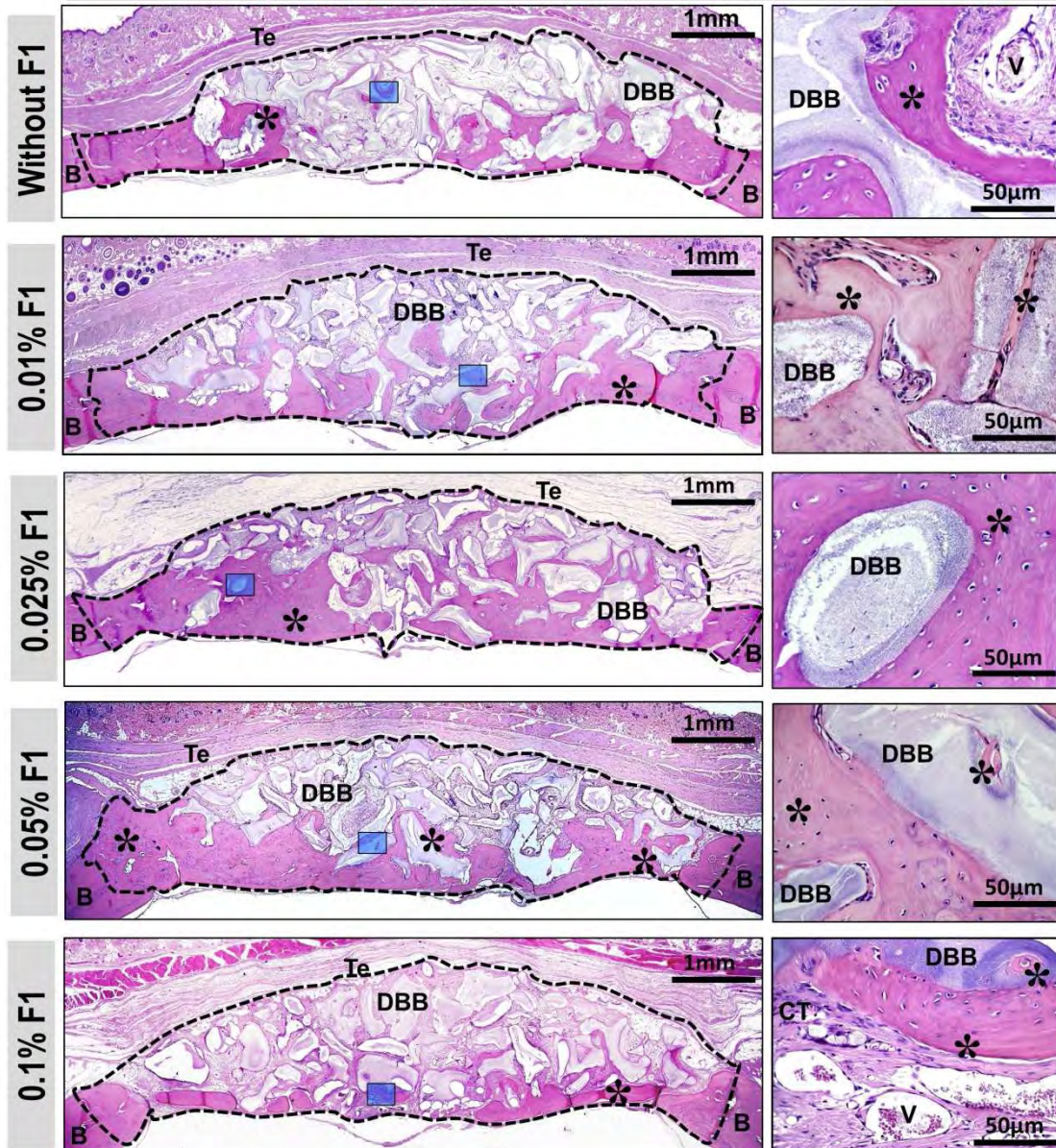
Sections	(C) Volume density or BV/TV (%)					
	pBCP70/30		New Bone		Soft tissue	
	Micro-CT	Histo	Micro-CT	Histo	Micro-CT	Histo
1	34.57	40.77	25.14	27.87	40.29	31.36
2	39.64	38.35	16.09	14.65	44.27	47.00
3	37.30	45.31	17.58	16.12	45.12	38.57
4	33.59	36.87	24.15	22.66	42.26	40.47
5	42.73	44.64	27.30	25.53	29.97	29.83
Mean ± SD	37.6 ± 2.9	41.2 ± 3.0	22.1 ± 4.2	21.4 ± 4.8	40.4 ± 4.2	37.4 ± 5.5
350 slice	36.1	-	23.6	-	40.3	-



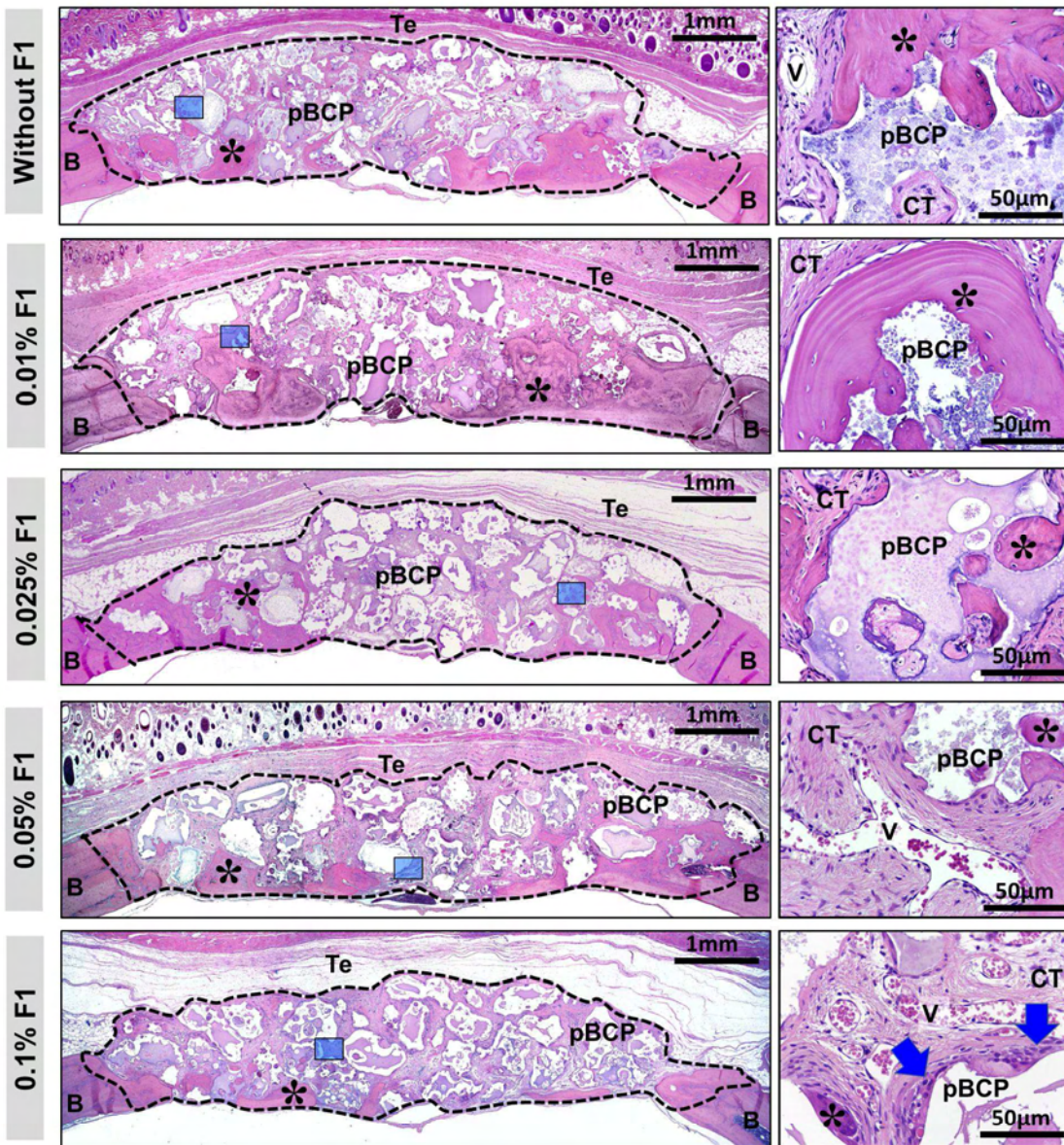
(A) Critical size bone defect (CSBD-CG)



(B) Deproteinized Bovine bone (DBB-TG)

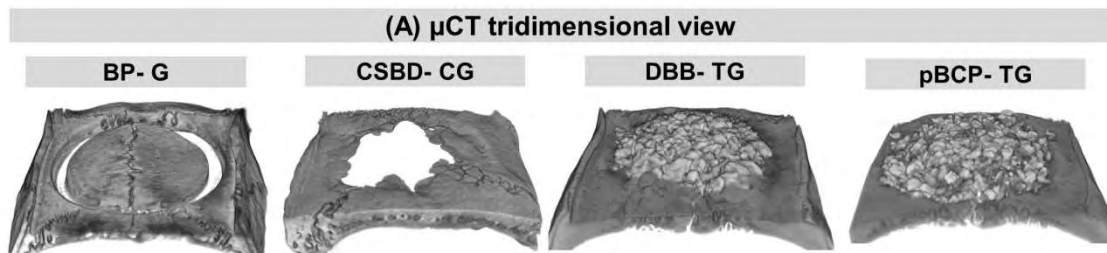


(A) Porous Biphasic calcium phosphate (pBCP-TG)

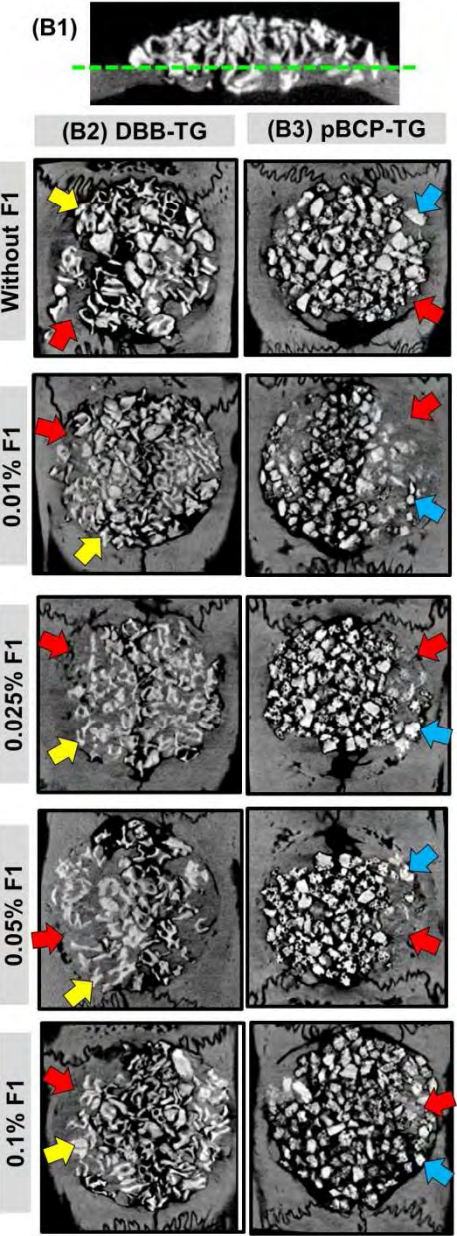


(B) Histological - Volume density (%)

F1	(B) Histological - Volume density (%)								
	(B1) Biomaterial			(B2) New Bone			(B3) Soft tissue		
	DBB	pBCP70/30	"t" Test (p)	DBB	pBCP70/30	"t" Test (p)	DBB	pBCP70/30	"t" Test (p)
Without	42.4 ± 2.1 ^A	45.9 ± 4.6 ^A	0.155	21.8 ± 3.7 ^A	18.0 ± 4.7 ^{A,B}	0.187	35.8 ± 2.4 ^{A,B}	36.1 ± 2.1 ^{A,B}	0.762
0.01%	41.7 ± 3.0 ^A	44.9 ± 2.7 ^A	0.500	24.7 ± 7.3 ^{A,B}	22.5 ± 6.8 ^B	0.629	33.6 ± 6.8 ^{A,B}	32.7 ± 6.9 ^A	0.671
0.025%	40.5 ± 2.8 ^A	43.1 ± 2.5 ^A	0.136	32.6 ± 5.4 ^B	19.3 ± 4.7 ^{A,B}	0.003 [#]	26.9 ± 3.6 ^B	37.6 ± 4.2 ^{A,B}	0.002 [#]
0.05%	40.2 ± 6.3 ^A	41.7 ± 3.0 ^A	0.434	25.1 ± 4.2 ^{A,B}	15.1 ± 4.0 ^{A,B}	0.005 [#]	34.8 ± 6.3 ^{A,B}	42.2 ± 5.0 ^{B,C}	0.075
0.1%	39.9 ± 3.7 ^A	40.0 ± 3.4 ^A	0.946	17.9 ± 5.7 ^A	13.2 ± 1.8 ^A	0.108	42.2 ± 3.7 ^A	46.8 ± 3.6 ^C	0.083
ANOVA (p)	0.8638	0.0854		0.0054	0.0274		0.0016	0.0008	



(B) μ CT bidimensional view



(C) μ CT morphometry - Total volume (mm³)

F1	(C1) Grafted region			(C2) Biomaterial		
	DBB-TG	pBCP-TG	"t" Test (p)	DBB-TG	pBCP-TG	"t" Test (p)
Without	83.2 $\pm 5.2^A$	88.7 $\pm 4.9^A$	0.119	36.7 $\pm 3.8^A$	40.7 $\pm 3.4^B$	0.049#
0.01%	85.0 $\pm 6.8^A$	89.6 $\pm 6.7^A$	0.313	35.4 $\pm 3.9^A$	40.1 $\pm 2.5^B$	0.030#
0.025%	88.8 $\pm 6.3^A$	89.1 $\pm 7.0^A$	0.942	36.0 $\pm 4.0^A$	38.5 $\pm 4.6^{A,B}$	0.389
0.05%	81.7 $\pm 2.6^A$	86.0 $\pm 4.0^{A,B}$	0.075	33.6 $\pm 5.1^A$	37.0 $\pm 3.3^{A,B}$	0.153
0.1%	80.4 $\pm 4.2^A$	77.1 $\pm 4.2^B$	0.254	32.1 $\pm 3.7^A$	31.6 $\pm 3.0^A$	0.852
ANOVA (p)	0.1417	0.0093		0.5776	0.0067	

F1	(C3) Bone tissue			(C4) Soft tissue		
	DBB-TG	pBCP-TG	"t" Test (p)	DBB-TG	pBCP-TG	"t" Test (p)
Without	18.43 $\pm 2.5^{A,C}$	15.9 $\pm 4.2^A$	0.281	30.6 $\pm 2.9^A$	32.1 $\pm 2.6^{B,C}$	0.228
0.01%	19.8 $\pm 3.6^{A,C}$	20.2 $\pm 6.3^A$	0.908	29.8 $\pm 5.3^A$	29.3 $\pm 6.6^{B,C}$	0.743
0.025%	29.7 $\pm 2.2^B$	17.2 $\pm 4.3^A$	0.000#	23.1 $\pm 4.1^B$	33.4 $\pm 3.7^C$	0.005#
0.05%	23.2 $\pm 3.3^{B,C}$	13.1 $\pm 2.8^A$	0.002#	25.3 $\pm 3.1^{A,B}$	36.7 $\pm 5.4^C$	0.037#
0.1%	14.4 $\pm 4.6^A$	10.4 $\pm 1.4^B$	0.102	33.9 $\pm 2.3^C$	37.5 $\pm 3.3^{B,C}$	0.118
ANOVA (p)	0.0001	0.0008		0.0006	0.0506	

Legends of illustrations

Figure 1 Scheme of the method used for obtaining F1-protein and incorporation on biomaterials: **A** extraction of latex and stabilization. **B** coagulation to obtaining serum fraction of the latex. **C** elevation of serum fraction pH to 9.0, determination of the final ionic strength and filtration, and **D** classical chromatography on DEAE-C (*Diethylaminoethyl cellulose*) and obtaining three protein sub-fractions with monitoring at 280nm in spectrophotometer. **E** processing and storage of the fractions; and **F** conduction of the F1 protein biomaterials bone substitutes.

Figure 2 Physico-chemical characterization. **A** SEM micrographs of DBB and pBCP70/30 show different shape, surface configuration and porosity of particles. **B** EDX spectra shows similar elemental chemical composition and Ca/P ratio between materials. **C** F1–Incorporation on the CaP-materials and F1-concentration implanted in the defect: a comparative analysis varying the concentrations of F1 to the materials implanted in the defects, showed that the material pBCP was more incorporated than the DBB.

Figure 3 Surgical procedures and 3D-microCT sagittal view of each experimental groups: **A** Skull rat show local and position of defect created in the parietal bones. **B** Critical-sized defect created with an 8-mm diameter trephine bur and bone plug. In the bone plug group (*BP-G*), the skull was collected immediately after surgery and the defects were used for determination of total volume of bone removed surgically or bone lost. **C** Defect filled with biomaterial without or plus F1 (*DBB-TG and pBCP-TG*). See detail shows material particles agglutinated with blood clot and standardization of biomaterial volume (60mm^3). **D** Defect filled only with blood clot (*CSBD-CG*).

Figure 4 Morphometric evaluations. **A** Morphometry in micro-CT coronal view using CTAn program: 3D-transaxial micro-CT view. **A₁** shows that all 350 slides/images of 2D coronal view between proximal (*blue dotted line*) and distal borders (*green dotted line*) were used for 3D morphometric evaluations. In the coronal slides. **A₂** show the regions of interest located between left (*LB*) and right (*RB*) borders of defect. Defect of *BP-G*. **A_{3a}** show ROI manual (*red area*) used for determination of total volume of bone removed

surgically at 0h. The defects of CSBD-CG. **A_{3b}** show the bone area automatically selected after binarizing of images (*red area*). The defect of treated groups shows. **A_{3c}** the biomaterials (*green areas*) and bone (*red areas*) after manual selection of grafted area and binarization. **B** Histomorphometry using AxioVision program: 3D-transaxial micro-CT view. **B₁** of CSBD-CG and treated group shows the regions of five histological sections selected per defect (*S1, S2, S3 and S5*). Note in the Figures **B₂** the histological sections of bone plug removed surgically of the each defect and in the defect of CSBD-CG. **B_{3a}** the total area evaluated represented by bone plug removed surgically (*area surrounded by black dotted line*). In the treated group **B_{3b}** the total area evaluated is the grafted region (*area surrounded by blue dotted line*). In the Figures **B₄** show the total area of bone (*red areas*) and biomaterial (*green areas*) manually selected for determination of volume density (%).

Figure 5 Comparative morphometric analysis between 2D-micro-CT slices and 2D-Histological sections in DBB-TG defect. **A-B** Five micro-CT coronal slices and similar histological sections show the ROI (*blue dotted line*) manually selected. Note in microCT images the DBB granules more hyperdense than bone tissue while in Histological sections the pBCP granules is represented by areas weak stained in purple (*hematoxylin*) and bone stained in magenta (*eosin*). **C** The Table show the values obtained for volume density of DBB granules, new bone and soft tissue for each slice/section. Observe that the mean values obtained for 2D-microCT slices are near to 2D-histological sections and the value obtained for 3D-micro-CT analysis evaluating a total of 350 slices; and **D1-D2** Graphics of Pearson correlation between 2D-micro-CT and 2D-Histological analysis show a strong correlation between methods and the p-value obtained in the paired t-test results show no statistical difference between methods.

Figure 6 Comparative morphometric analysis between 2D-micro-CT slice and 2D-Histological sections in pBCP-TG defect. **A-B** Five micro-CT coronal slices and similar histological sections show the ROI (*blue dotted line*) manually selected. Similar to observe in DBB-TG, the microCT images of pBCP granules show more hyperdense than bone tissue and in histological sections the DBB granules is represented by areas weak stained in purple (*hematoxylin*) and bone stained in magenta (*eosin*). **C** The Table show the

values obtained for volume density of pBCP granules, new bone and soft tissue for each slice/section. Observe that the mean values obtained for bone in 2D-microCT slices are near to 2D-histological and 3D-micro-CT analysis, but a greater variability is observed for biomaterial; and **D1-D2** Graphics of Pearson correlation between 2D-micro-CT and 2D-Histological analysis show a moderated to weak correlation between methods for pBCP volume density and strong correlation for new bone. The p-value obtained in the paired t-test results show no statistical difference between methods.

Figure 7 Histological view of bone defects of CSBD-CG **A** and DBB-TG **B**. **A** CSBD-CG bone defect show small bone formation (asterisk) in the border, and the remaining defect filled by fibrous connective tissue (CT) and tegument tissues (Te); and **B** DBB-TG defects show similar grafted area (*area surrounded black dotted line*). In DBB-TG without F1 the bone formation is present in the defect border surrounding some granules near to dura mater surface. Detail show small bone formation on DBB surface and connective tissue (CT) filling the remaining space between DBB granules. An increase of bone formation (*asterisks*) can be observed when DBB was incorporating with F1 at concentration of 0.025% and 0.05%. In these concentrations, most of the dura mater surface and of the spaces between the granules are filled by compact bone tissue (*asterisk*). Details show, the entrapment of the DBB granules within the neoformed bone (*asterisk*). The incorporation of 0.1% F1 into DBB shows a negative effect on bone formation. Detail show small bone formation (*asterisk*) on DBB surface and presence of anomalous macrovessels (V) in the connective tissue (CT) that filling the spaces between granules. HE, x4 and x40 objectives.

Figure 8 Histological view of bone defect of pBCP-TG. **A** All bone defects show similar grafted area (*area surrounded black dotted line*). The defects of pBCP-TG without F1 show small bone formation in its border surrounding some granules near to dura mater surface. Detail show small bone formation on irregular surface of pBCP and connective tissue (CT) occupying the spaces between granules. A small increase of bone formation (*asterisks*) can be observed only when pBCP was incorporating with F1 at concentration of 0.01%. Detail show bone tissue surrounding a pBCP granule. Concentrations of more than 0.01% F1 show a proportional negative effect on the bone formation. Detail show small bone formation (*asterisk*)

and foreign body giant cells (FBGCs) on pBCP surface, and anomalous macrovessels (V) in the connective tissue (CT) that filling the spaces between granules. HE, x4 and x40 objectives. **B** Morphometric comparison of different concentrations of F1 and carriers: the table show mean and SD obtained for volume density of Biomaterials **B₁**, New Bone **B₂** and soft tissue **B₃** in the defects of treated groups. Statistically, the bone formation **B₂** was higher when DBB was incorporated with 0.025%F1. Different letters = statistical differences between F1 concentration (*Tukey test after one-way ANOVA*); and symbol = differences between carriers/materials (*"t" test*).

Figure 9 μ CT evaluations. **A** 3D images of experimental groups show bone block into defect of BP-G after trephination, absence of mineralized bone in the central region of defect in CSBD-CG and granules of the carrier biomaterial filling the entire defect in DBB-TG and pBCP-TG. **B** 2D-coronal image show the plane used to obtain transaxial images of defect near to dura-mater region **B₁**. DBB-TG **B₂** and pBCP-TG **B₃** defects show the new bone formation (*red arrow*) in the defect border and in the spaces between the granules (*yellow arrow*). Note higher new bone formation in DBB incorporated with 0.025% and 0.05% of F1 and pBCP incorporated with 0.01%F1. **C** Table of volumetric assessment of grafted region **C₁**, biomaterials granules **C₂**, new bone formation **C₃** and soft tissue show differences statistically significant in relation to concentration of F1 incorporated on materials and carrier material. Different letters = statistical differences between F1 concentration (*Tukey test after one-way ANOVA*); and symbol = differences between carriers/materials (*"t" test*).

4 DISCUSSION

4 DISCUSSION

Bone regeneration is a complex and dynamic biological process involving cellular and molecular elements during the new bone formation (Ai-Aql *et al.*, 2008). However, large bone defects remain a clinical challenge, pathological situations or trauma, may compromise the healing process of the repair (Gómez-Barrena *et al.*, 2015; Panteli *et al.*, 2015). Another crucial factor for a good healing is that the damaged bone location needs to be highly vascularized (Portal-Núñez *et al.*, 2012; Hu and Olsen, 2016; 2017). Additionally, current strategies for tissue engineering developed therapies with growth factors associated to bone grafts attempting to induce new vessels formation then they could be good alternatives because they can provide oxygen, nutrients, and promote direct migration to bone defects (Gorustovich *et al.*, 2010). In this context angiogenesis is closely linked to a better bone formation and we studied latex F1 protein performance versus 2 different bone biomaterials. Recently, the experimental model most commonly used to evaluate bone replacement strategies has been in calvaria of rats (Vajgel *et al.*, 2014), based on the critical size defect (Cooper *et al.*, 2010). Schmitz & Hollinger (1986), gave rise to the term "Critical Size Defect" (CSBD), defined as a defect that lacks the natural repair capability during the life of the animal. In our study, was performed in calvaria of the rat a creating a unilateral defect of 8-mm of diameter. A other pilot study carried out in our laboratory showed spontaneous healing of a 5-mm bone defect in adult rats leading to closed of defect ($47.5 \pm 9.8\%$ at 12 weeks and $83.3 \pm 13.1\%$ at 24 weeks, data not included) considered as a subcritical size defect that can heal without intervention. Other study, also showed that bilateral defects of 5mm in association with the application of factors of growth, the control site may be contaminated due to defects being near (Vajgel *et al.*, 2014).

The methods used to verify bone repair in these experimental models include histological and histomorphometric evaluations (Park *et al.*, 2009), because this technique is considered gold standard (Vidal *et al.*, 2012) and allows to evaluate elements present in the tissue samples by means of two-dimensional cuts, qualitatively and quantitatively. Therefore, it is not possible to evaluate the sample volume, requiring three-dimensional samples (Li *et al.*, 2010). In order to complement the method of histological quantification, we associate to the morphometric method the computerized microtomography, allowing the obtaining of the three-dimensional samples (Efeoglu *et al.*, 2007; Parkinson *et al.*, 2008), being a new technique with many advantages, among them: the ability to evaluate several parameters depending on the

software and hardware it has, does not damage the sample, ensuring the integrity of the sample for other techniques used later (Ho and Hutmacher, 2006) and considered the safest method in quantitative analysis (Gundersen *et al.*, 1988). Although, it has the disadvantage of the microtomographic analysis of bone tissue, the program makes it impossible to change the gray levels during quantification of bone volume (Parkinson *et al.*, 2008). Many studies have used two techniques and have done compared microtomographic and histomofometric data (Yeom *et al.*, 2008; Particelli *et al.*, 2012).

In the present study, some difficulties were found during quantifications correlation between 2D-micro-CT morphometry and histomorphometry measures. The values obtained were discordant between both analyzes and similar difficulties are also found in the work of Chappard *et al.*, (2005). Most of the methodologies only evaluate a single region of the graft, in this regard, taking into account that the bone repair does not occur simultaneously in the whole defect, we had the idea of creating a new methodology of stratified analysis considering the whole region and also performing comparisons between similar micro-CT and histological cuts. Since there are no studies that use these methodology thresholds were standardized and after segmentation we had the following analyzes: volume of density (Vv), new bone (Vv-NB), biomaterials (Vv-DBB e Vv-pBCP), bone marrow (Vv-MB) and soft tissue (Vv -ST) in the CTAn program for the microCT samples, and in the AxionVision program, in the histological samples.

The findings showed that, there was no statistical difference between the mean values of volumetric density of the bone tissue, biomaterial and soft tissue, obtained in micro-CT and histological images (Figs. 5D2 e 6D2) e DBB (Fig. 6D1). Regarding histomorphometry the CSBD group, a small bone formation occurred, being $20.7 \pm 8.2\%$, considered a critical-size defect. Regarding the treatment groups, the implanted volume remained stable over the period of 120 days in both groups. However, a volume loss of the pBCP (Table of the Fig. 8B), associated with the appearance of multinucleate foreign body giant cells (FBGCs, see Fig. 8A) at concentrations of 0.05% and 0.1% F1. Recent studies have shown that the presence of FBGCs found on the surface of calcium phosphate ceramics is correlated with increased vascularity in tissue repair, considering important the vascular endothelial growth factor (VEGF) during bone formation (Ghanaati *et al.*, 2010) (Yang *et al.*, 2012). However, in our work the presence of FBGCs was associated with the presence of anomalous microspheres, verified in concentrations above 0.05% F1. Experimental data have shown that the application of excessive amounts of growth

factors causes irregular blood vessels to appear (Zisch *et al.*, 2003; Davies *et al.*, 2008). Moreover, pathologies of angiogenesis may occur (Moldovan and Moldovan, 2002), as seen, the dosage of VEGF should be strictly controlled (Davies *et al.*, 2008). Considering the importance of the dosage of these growth factors when associated with biomaterials in tissue engineering, other studies have investigated the release of these drugs (Liu *et al.*, 2013; Li *et al.*, 2015).

Highlighting a link, the characteristics of the biomaterials to be proposed in therapy, such as pore sizes, chemical and physical properties as some studies have done, should be taken into account. (Klein *et al.*, 1984; Hamada *et al.*, 2010; Otsuka *et al.*, 2013; Ebrahimi and Botelho, 2017; Ebrahimi *et al.*, 2017). For this reason, we performed the characterization of the biomaterials carried to F1 (Fig. 2), verifying the properties of the ceramics pBCP and DBB. The analysis showed morphology, porosity of the different granules between one material and another. And there was a relationship between the Ca / P elements 1.66 and 1.67 in both materials. On the other hand, the solubility of the material may also interfere with the regeneration process. In this context, (Ghanaati *et al.*, 2012), used in its study pure HA and TCP granules and associated HA / TCP, in the proportion 60:40, analyzing action when used pure and associated, after the experiment period being of up to 30 days, the results showed that, when using pure ceramics, the TCP was absorbed faster to the connective tissue, presence of multinucleated giant cells and an intense vascularization, already HA, presented the opposite, a slow degradation, few multinucleated giant cell cells. That is, when used in conjunction, HA / TCP 60/30, the ceramic presents an equilibrium between the vascularization and the degradation of the material, being an excellent combination to restore the bone tissue. In relation to HA / TCP in the ratio 70:30, used in our work, in the study of (Lomelino *et al.*, 2012), showed that 70:30 biphasic pottery ceramics an increase in bone repair, and presented similar characteristics to the autogenous bone, such as bone tissue cells. These synthetic ceramics are largely research and studies show to be biocompatible, osteoconductive and allow the formation of a new bone on its surface (Damien and Parsons, 1991; Hak, 2007)

Concerning DBB ceramics, in our study pottery promoted good osseointegration of DBB as well as pBCP (Details in the Fig. 7B), the total volume of region grafted on DBB-TG and pBCP-TG (Table in the Fig. 9C) was 99,8% bigger (average of 85 mm³) than surgically removed, with an average of 42,6 mm³. It was also observed direct communication of the new bone and the surface of the material without interposition of soft tissue. In study of Cestari *et al.* 2009, we can see the similarity to our results, study was carried out with the sintered bovine-derived anorganic bone material (sBDAB) as in form of block in the repair of a bone defect of

critical size and observed that it promoted excellent osseointegration from the edges of the defects towards the center, bone volume was 3.8 times greater compared to surgically removed bone, whereas in the control group, filled only with the blood clot of the animal itself, bone formation was limited. They concluded that the DBB block possesses osteoconductive property, block providing osteoconductive, a slow reabsorption and osteoconductive. In the study of Rocha et al. (2011), evaluated the Gen-Ox®inorg associated with and without the platelet-rich plasma (PRP), after the 4-week experimental period, observed the presence of a small bone formation in edge region and in some defects was observed in central region, was seen the presence of giant cells in the group Gen-Ox®inorg without and with the PRP, where they concluded that in addition to being osteoinductive, it maintains the new bone volume.

Given the evidences found here, we can say that biomaterials are well accepted in the literature, and are closely linked to growth factors. In this way, the results presented in this study showed the potential of F1 carried to the biomaterials, being dose dependent and the choice of biomaterial can also be influenced. in addition, new methodologies proposed in this work using the combination 2D/3D micro-CT and histomorphometric analysis to evaluate bone regeneration could help future studies in a calvary model of critical size in rats.

5 CONCLUSIONS

5 CONCLUSIONS

Our study demonstrates that the potential of F1 in stimulating angiogenesis and osteogenesis is dependent on the concentration and carrier biomaterial. In the other hand, we present a new methodology standardized in this study using the combination 2D/3D micro-CT and histomorphometric analysis for future preclinical studies in critical size defect as an experimental model in rat calvaria, in bone regeneration.

REFERENCES

REFERENCES

- AGRAWAL, V.; SINHA, M. A review on carrier systems for bone morphogenetic protein-2. **J Biomed Mater Res B Appl Biomater**, Jan 2016. ISSN 1552-4981 (Eletronic)
- AI-AQL, Z. S. et al. Molecular mechanisms controlling bone formation during fracture healing and distraction osteogenesis. **J Dent Res**, v. 87, n. 2, p. 107-18, Feb 2008. ISSN 0022-0345 (Eletronic)
- ARAUJO, M. M.; MASSUDA, E. T.; HYPPOLITO, M. A. Anatomical and functional evaluation of tympanoplasty using a transitory natural latex biomembrane implant from the rubber tree *Hevea brasiliensis*. **Acta Cir Bras**, v. 27, n. 8, p. 566-71, Aug 2012. ISSN 1678-2674 (Eletronic)
- BALABANIAN, C. A. et al. Biocompatibility of natural latex implanted into dental alveolus of rats. **J Oral Sci**, v. 48, n. 4, p. 201-5, Dec 2006. ISSN 1343-4934 (Eletronic)
- CAMPANA, V. et al. Bone substitutes in orthopaedic surgery: from basic science to clinical practice. **J Mater Sci Mater Med**, v. 25, n. 10, p. 2445-61, Oct 2014. ISSN 1573-4838 (Eletronic)
- CANCEDDA, R.; GIANNONI, P.; MASTROGIACOMO, M. A tissue engineering approach to bone repair in large animal models and in clinical practice. **Biomaterials**, v. 28, n. 29, p. 4240-50, Oct 2007. ISSN 0142-9612 (Eletronic)
- CARRAGEE, E. J. et al. Cancer risk after use of recombinant bone morphogenetic protein-2 for spinal arthrodesis. **J Bone Joint Surg Am**, v. 95, n. 17, p. 1537-45, Sep 2013. ISSN 1535-1386 (Eletronic)
- CARREIRA, A. C. et al. Bone morphogenetic proteins: facts, challenges, and future perspectives. **J Dent Res**, v. 93, n. 4, p. 335-45, Apr 2014. ISSN 1544-0591 (Eletronic)
- CESTARI, T. M. et al. Bone repair and augmentation using block of sintered bovine-derived anorganic bone graft in cranial bone defect model. **Clin Oral Implants Res**, v. 20, n. 4, p. 340-50, Apr 2009. ISSN 1600-0501 (Eletronic)
- CHIN, M. et al. Repair of alveolar clefts with recombinant human bone morphogenetic protein (rhBMP-2) in patients with clefts. **J Craniofac Surg**, v. 16, n. 5, p. 778-89, Sep 2005. ISSN 1049-2275 (Eletronic)
-
-

COOPER, G. M. et al. Testing the critical size in calvarial bone defects: revisiting the concept of a critical-size defect. *Plast Reconstr Surg*, v. 125, n. 6, p. 1685-92, Jun 2010. ISSN 1529-4242 (Eletronic)

DAMIEN, C. J.; PARSONS, J. R. Bone graft and bone graft substitutes: a review of current technology and applications. *J Appl Biomater*, v. 2, n. 3, p. 187-208, 1991. ISSN 1045-4861 (Eletronic)

DAVIES, N. et al. The dosage dependence of VEGF stimulation on scaffold neovascularisation. *Biomaterials*, v. 29, n. 26, p. 3531-8, Sep 2008. ISSN 0142-9612 (Eletronic)

EBRAHIMI, M.; BOTELHO, M. Biphasic calcium phosphates (BCP) of hydroxyapatite (HA) and tricalcium phosphate (TCP) as bone substitutes: Importance of physicochemical characterizations in biomaterials studies. *Data Brief*, v. 10, p. 93-97, Feb 2017. ISSN 2352-3409 (Eletronic)

EBRAHIMI, M.; BOTELHO, M. G.; DOROZHKIN, S. V. Biphasic calcium phosphates bioceramics (HA/TCP): Concept, physicochemical properties and the impact of standardization of study protocols in biomaterials research. *Mater Sci Eng C Mater Biol Appl*, v. 71, p. 1293-1312, Feb 2017. ISSN 1873-0191 (Eletronic)

EFEOGLU, C. et al. Quantitative morphometric evaluation of critical size experimental bone defects by microcomputed tomography. *Br J Oral Maxillofac Surg*, v. 45, n. 3, p. 203-7, Apr 2007. ISSN 0266-4356 (Eletronic)

FRADE, M. C. et al. Management of diabetic skin wounds with a natural latex biomembrane. *Med Cutan Iber Lat Am*, v. 32, n. 4, p. 157-62, 2004 (Eletronic)

GHANAATI, S. et al. The chemical composition of synthetic bone substitutes influences tissue reactions in vivo: histological and histomorphometrical analysis of the cellular inflammatory response to hydroxyapatite, beta-tricalcium phosphate and biphasic calcium phosphate ceramics. *Biomed Mater*, v. 7, n. 1, p. 015005, Feb 2012. ISSN 1748-605X (Eletronic)

_____. Influence of β -tricalcium phosphate granule size and morphology on tissue reaction in vivo. *Acta Biomater*, v. 6, n. 12, p. 4476-87, Dec 2010. ISSN 1878-7568 (Eletronic)

GORUSTOVICH, A. A.; ROETHER, J. A.; BOCCACCINI, A. R. Effect of bioactive glasses on angiogenesis: a review of in vitro and in vivo evidences. *Tissue Eng Part B Rev*, v. 16, n. 2, p. 199-207, Apr 2010. ISSN 1937-3376 (Eletronic)

GUNDERSEN, H. J. et al. Some new, simple and efficient stereological methods and their use in pathological research and diagnosis. *APMIS*, v. 96, n. 5, p. 379-94, May 1988. ISSN 0903-4641(Eletronic)

GÓMEZ-BARRENA, E. et al. Bone fracture healing: cell therapy in delayed unions and nonunions. *Bone*, v. 70, p. 93-101, Jan 2015. ISSN 1873-2763(Eletronic)

HAK, D. J. The use of osteoconductive bone graft substitutes in orthopaedic trauma. *J Am Acad Orthop Surg*, v. 15, n. 9, p. 525-36, Sep 2007. ISSN 1067-151X (Eletronic)

HAMADA, H. et al. Effect of geometrical structure on the biodegradation of a three-dimensionally perforated porous apatite/collagen composite bone cell scaffold. *Biol Pharm Bull*, v. 33, n. 7, p. 1228-32, 2010. ISSN 1347-5215 (Eletronic)

HO, S. T.; HUTMACHER, D. W. A comparison of micro CT with other techniques used in the characterization of scaffolds. *Biomaterials*, v. 27, n. 8, p. 1362-76, Mar 2006. ISSN 0142-9612 (Eletronic)

HU, K.; OLSEN, B. R. The roles of vascular endothelial growth factor in bone repair and regeneration. *Bone*, v. 91, p. 30-8, 10 2016. ISSN 1873-2763 (Eletronic)

_____. Vascular endothelial growth factor control mechanisms in skeletal growth and repair. *Dev Dyn*, v. 246, n. 4, p. 227-234, 04 2017. ISSN 1097-0177 (Eletronic)

ISSA, J. P. et al. Biological evaluation of the bone healing process after application of two potentially osteogenic proteins: an animal experimental model. *Gerodontology*, v. 29, n. 4, p. 258-64, Dec 2012. ISSN 1741-2358 (Eletronic)

KLEIN, C. P.; DRIESSEN, A. A.; DE GROOT, K. Relationship between the degradation behaviour of calcium phosphate ceramics and their physical-chemical characteristics and ultrastructural geometry. *Biomaterials*, v. 5, n. 3, p. 157-60, May 1984. ISSN 0142-9612 (Eletronic)

Lamounier, F. Avaliação da produção de citocinas inflamatórias "in vitro", induzidas pela membrana de látex natural seringueira *Havea Brasiliensis*, 115. Mestrado. Departamento de Clínica Médica, Divisão de Dermatologia, Faculdade de Medicina de Ribeirão Preto, Univerdade de São Paulo, Ribeirão Preto, 2004.

LAURENCIN, C.; KHAN, Y.; EL-AMIN, S. F. Bone graft substitutes. *Expert Rev Med Devices*, v. 3, n. 1, p. 49-57, Jan 2006. ISSN 1743-4440 (Eletronic)

LI, L. et al. Controlled dual delivery of BMP-2 and dexamethasone by nanoparticle-embedded electrospun nanofibers for the efficient repair of critical-sized rat calvarial defect. *Biomaterials*, v. 37, p. 218-29, Jan 2015. ISSN 1878-5905 (Eletronic)

LI, W. et al. Nell-1 enhances bone regeneration in a rat critical-sized femoral segmental defect model. *Plast Reconstr Surg*, v. 127, n. 2, p. 580-7, Feb 2011. ISSN 1529-4242 (Eletronic)

LI, X. et al. Osteogenic induction of adipose-derived stromal cells: not a requirement for bone formation in vivo. *Artif Organs*, v. 34, n. 1, p. 46-54, Jan 2010. ISSN 1525-1594 (Eletronic)

LIU, T. et al. Deproteinized bovine bone functionalized with the slow delivery of BMP-2 for the repair of critical-sized bone defects in sheep. *Bone*, v. 56, n. 1, p. 110-8, Sep 2013. ISSN 1873-2763 (Eletronic)

LIU, W. C. et al. Angiogenesis Assays for the Evaluation of Angiogenic Properties of Orthopaedic Biomaterials - A General Review. *Adv Healthc Mater*, v. 6, n. 5, Mar 2017 (Eletronic)

LIU, Y. et al. Segmental bone regeneration using an rhBMP-2-loaded gelatin/nanohydroxyapatite/fibrin scaffold in a rabbit model. *Biomaterials*, v. 30, n. 31, p. 6276-85, Oct 2009. ISSN 1878-5905 (Eletronic)

LOMELINO, R. E. O. et al. The association of human primary bone cells with biphasic calcium phosphate (β TCP/HA 70:30) granules increases bone repair. *J Mater Sci Mater Med*, v. 23, n. 3, p. 781-8, Mar 2012. ISSN 1573-4838 (Eletronic)

MACHADO, E. G. et al. A new heterologous fibrin sealant as scaffold to recombinant human bone morphogenetic protein-2 (rhBMP-2) and natural latex proteins for the repair of tibial bone defects. *Acta Histochem*, v. 117, n. 3, p. 288-96, Apr 2015. ISSN 1618-0372 (Eletronic)

MANFRIN ARNEZ, M. F. et al. Implant osseointegration in circumferential bone defects treated with latex-derived proteins or autogenous bone in dog's mandible. *Clin Implant Dent Relat Res*, v. 14, n. 1, p. 135-43, Mar 2012. ISSN 1708-8208 (Eletronic)

MARENZANA, M.; ARNETT, T. R. The Key Role of the Blood Supply to Bone. *Bone Res*, v. 1, n. 3, p. 203-15, Sep 2013. ISSN 2095-4700 (Eletronic)

MAURÍCIO, V. Aceleração do reparo tissular induzido por uma fração angiogênica purificada do látex natural da seringueira *Hevea brasiliensis*. 2006. 111 p. Dissertação

(Mestrado em Medicina) – Faculdade de Medicina, Universidade de São Paulo, Ribeirão Preto

MENDONÇA, R.J. Caracterização biológica de uma fração angiogênica do latex natural da seringueira *Hevea brasiliensis*. Dissertação de Mestrado. FMRP-USP, Ribeirão Preto, 2004.

MENDONÇA, R. J. et al. Increased vascular permeability, angiogenesis and wound healing induced by the serum of natural latex of the rubber tree *Hevea brasiliensis*. **Phytother Res**, v. 24, n. 5, p. 764-8, May 2010. ISSN 1099-1573 (Eletronic)

MOLDOVAN, L.; MOLDOVAN, N. I. Trends in genomic analysis of the cardiovascular system. *Arch Pathol Lab Med*, v. 126, n. 3, p. 310-6, Mar 2002. ISSN 0003-9985(Eletronic)

MOORE, W. R.; GRAVES, S. E.; BAIN, G. I. Synthetic bone graft substitutes. **ANZ J Surg**, v. 71, n. 6, p. 354-61, Jun 2001. ISSN 1445-1433 (Eletronic)

MRUE, F. et al. Evaluation of the biocompatibility of a new biomembrane. **Materials Research**, v. 7, n. 2, p. 277-283, 2004. ISSN 1516-1439.

OTSUKA, M. et al. Effect of geometrical structure on the in vivo quality change of a three-dimensionally perforated porous bone cell scaffold made of apatite/collagen composite. *J Biomed Mater Res B Appl Biomater*, v. 101, n. 2, p. 338-45, Feb 2013. ISSN 1552-4981 (Eletronic)

PANTELI, M. et al. Biological and molecular profile of fracture non-union tissue: current insights. *J Cell Mol Med*, v. 19, n. 4, p. 685-713, Apr 2015. ISSN 1582-4934 (Eletronic)

PARK, J. W. et al. Bone formation with various bone graft substitutes in critical-sized rat calvarial defect. *Clin Oral Implants Res*, v. 20, n. 4, p. 372-8, Apr 2009. ISSN 1600-0501 (Eletronic)

PARKINSON, I. H.; BADIEI, A.; FAZZALARI, N. L. Variation in segmentation of bone from micro-CT imaging: implications for quantitative morphometric analysis. *Australas Phys Eng Sci Med*, v. 31, n. 2, p. 160-4, Jun 2008. ISSN 0158-9938 (Eletronic)

PARTICELLI, F. et al. A comparison between micro-CT and histology for the evaluation of cortical bone: effect of polymethylmethacrylate embedding on structural parameters. *J Microsc*, v. 245, n. 3, p. 302-10, Mar 2012. ISSN 1365-2818 (Eletronic)

PORTAL-NÚÑEZ, S.; LOZANO, D.; ESBRIT, P. Role of angiogenesis on bone formation. *Histol Histopathol*, v. 27, n. 5, p. 559-66, 05 2012. ISSN 1699-5848 (Eletronic)

ROCHA, C. A. Avaliação comparativa da neoformação óssea após enxertia de HA/TCPp, Bio-Oss e osso autógeno associados ou não ao PRP em cirurgias de levantamento de seio maxilar de coelhos 2015. 158 Universidade de São Paulo. Faculdade de Odontologia de Bauru

SANTOS, A. A. D. et al. The role of bone morphogenetic protein on bone tissue repair. **Acta Ortopédica Brasileira**, v. 13, n. 4, p. 194-195, 2005. ISSN 1413-7852.

SANTOS, P. S. et al. Osteoinductive porous biphasic calcium phosphate ceramic as an alternative to autogenous bone grafting in the treatment of mandibular bone critical-size defects. **J Biomed Mater Res B Appl Biomater**, v. 106, n. 4, p. 1546-1557, May 2018. ISSN 1552-4981 (Eletronic)

SCHMITZ, J. P.; HOLLINGER, J. O. The critical size defect as an experimental model for craniomandibulofacial nonunions. *Clin Orthop Relat Res*, n. 205, p. 299-308, Apr 1986. ISSN 0009-921X (Eletronic)

TADIC, D.; EPPLE, M. A thorough physicochemical characterisation of 14 calcium phosphate-based bone substitution materials in comparison to natural bone. **Biomaterials**, v. 25, n. 6, p. 987-94, Mar 2004. ISSN 0142-9612 (Eletronic)

TORIUMI, D. M.; ROBERTSON, K. Bone inductive biomaterials in facial plastic and reconstructive surgery. **Facial Plast Surg**, v. 9, n. 1, p. 29-36, Jan 1993. ISSN 0736-6825 (Eletronic)

VAJGEL, A. et al. A systematic review on the critical size defect model. *Clin Oral Implants Res*, v. 25, n. 8, p. 879-93, Aug 2014. ISSN 1600-0501 (Eletronic)

VIDAL, B. et al. Bone histomorphometry revisited. *Acta Reumatol Port*, v. 37, n. 4, p. 294-300, 2012 Oct-Dec 2012. ISSN 0303-464X (Eletronic)

YANG, Y. Q. et al. The role of vascular endothelial growth factor in ossification. *Int J Oral Sci*, v. 4, n. 2, p. 64-8, Jun 2012. ISSN 1674-2818 (Eletronic)

YEOM, H. et al. Correlation between micro-computed tomography and histomorphometry for assessment of new bone formation in a calvarial experimental model. *J Craniofac Surg*, v. 19, n. 2, p. 446-52, Mar 2008. ISSN 1049-2275 (Eletronic)

ZIMMERER, R. M. et al. In vivo tissue engineered bone versus autologous bone: stability and structure. **Int J Oral Maxillofac Surg**, v. 46, n. 3, p. 385-393, Mar 2017. ISSN 1399-0020 (Electronic)

ZISCH, A. H.; LUTOLF, M. P.; HUBBELL, J. A. Biopolymeric delivery matrices for angiogenic growth factors. *Cardiovasc Pathol*, v. 12, n. 6, p. 295-310, 2003 Nov-Dec 2003. ISSN 1054-8807 (Electronic)

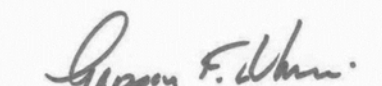
APPENDIX

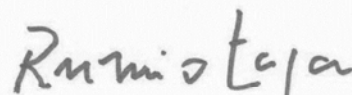
**DECLARATION OF EXCLUSIVE USE OF THE ARTICLE
IN DISSERTATION**

We hereby declare that we are aware of the article "*F1 protein fraction obtained from latex incorporated into CaP-materials improve critical-size defect bone repair in a concentration-dependent manner*" will be included in Dissertation of the student **Suelen Pains** and can not be used in other works of the Graduate Programs of the Faculty of Dentistry of Bauru of the University of São Paulo.

Bauru, 7 de Agosto de 2018.


Suelen Pains


Gerson Francisco de Assis


Rumio Taga

ANNEXS

ANNEXS



Universidade de São Paulo
Faculdade de Odontologia de Bauru



CERTIFICADO

CERTIFICAMOS que a proposta intitulada "*Biocompatibilidade e o potencial angiogênico e osteogênico da proteína angiogênica F1 purificada do látex natural e associada a diferentes carreadores*", registrada sob nº **CEEPA Proc. nº 027/2011**, sob a responsabilidade do Prof. Dr. Rumio Taga, que envolveu a utilização de animais pertencentes ao filo *Chordata*, subfilo *Vertebrata* (exceto humanos), para fins de pesquisa científica, encontra-se de acordo com os preceitos da Lei nº 11.794, de 8 de outubro de 2008, do Decreto nº 6.899, de 15 de julho de 2009, e com as normas editadas pelo Conselho Nacional de Controle de Experimentação Animal (CONCEA), e foi **aprovada** em reunião ordinária da Comissão de Ética no Ensino e Pesquisa em Animais (CEEPA), da Faculdade de Odontologia de Bauru-USP, realizada no dia 14 de março de 2017.

Finalidade	() Ensino (X) Pesquisa Científica
Vigência da autorização	Agosto/2011 a Agosto/2012
Espécie/Linhagem	<i>Rattus norvegicus</i> , Wistar
Nº de animais	N=180
Peso/Idade	60 animais com aproximadamente 200g 120 animais com aproximadamente 350g
Sexo	Machos
Origem	Biotério de Criação ANILAB/Paulínia, SP

21 de março de 2017.

Data



Profª Drª Ana Paula Campanelli
Presidente da Comissão de Ética no Ensino e Pesquisa em Animais



CEEPA
Comissão de Ética no Ensino e Pesquisa em Animais



Universidade de São Paulo Faculdade de Odontologia de Bauru

Comissão de Ética no Ensino e Pesquisa em Animais

CEEPA-Proc. Nº 004/2017.

Bauru, 5 de maio de 2017.

Senhor Professor,

Informamos que Projeto de Pesquisa denominado *"Influência da concentração da proteína F1 purificada do látex natural (Heve brasiliensis) e do biomaterial carreador na vascularização e formação óssea em defeitos ósseos cranianos de tamanho crítico. Estudo microtomográfico, histomofométrico e imunistoquímico"* tendo Vossa Senhoria como Pesquisador Responsável, que envolve a utilização de animais (roedores), para fins de pesquisa científica, encontra-se de acordo com os preceitos da Lei nº 11.794, de 8 de outubro de 2008, do Decreto nº 6.899, de 15 de julho de 2009, e com as normas editadas pelo Conselho Nacional de Controle da Experimentação Animal (CONCEA), foi analisado e considerado APROVADO em reunião ordinária da Comissão de Ética no Ensino e Pesquisa em Animais (CEEPA), realizada nesta data.

Vigência do projeto:	<i>Maio/2017 a Abril/2019</i>
Espécie/Linhagem:	<i>Amostras biológicas (calvária de ratos incluídos em Histosec-Merck) provenientes do protocolo CEEPA 027/2011</i>
Nº de animais:	<i>Não se aplica</i>
Peso/Idade	<i>Não se aplica</i>
Sexo:	<i>Não se aplica</i>
Origem:	<i>Não se aplica</i>

Esta CEEPA solicita que ao final da pesquisa seja enviado um Relatório com os resultados obtidos para análise ética e emissão de parecer final, o qual poderá ser utilizado para fins de publicação científica.

Atenciosamente,

Profª Drª Ana Paula Campanelli

Presidente da Comissão de Ética no Ensino e Pesquisa em Animais

Prof. Dr. Gerson Francisco de Assis
Docente do Departamento de Ciências Biológicas